

REVIEW

Open Access



# Nanomaterials meet surface-enhanced Raman scattering towards enhanced clinical diagnosis: a review

Kaisong Yuan<sup>1,2</sup>, Beatriz Jurado-Sánchez<sup>2,3\*</sup> and Alberto Escarpa<sup>2,3\*</sup>

## Abstract

Surface-enhanced Raman scattering (SERS) is a very promising tool for the direct detection of biomarkers for the diagnosis of i.e., cancer and pathogens. Yet, current SERS strategies are hampered by non-specific interactions with co-existing substances in the biological matrices and the difficulties of obtaining molecular fingerprint information from the complex vibrational spectrum. Raman signal enhancement is necessary, along with convenient surface modification and machine-based learning to address the former issues. This review aims to describe recent advances and prospects in SERS-based approaches for cancer and pathogens diagnosis. First, direct SERS strategies for key biomarker sensing, including the use of substrates such as plasmonic, semiconductor structures, and 3D order nanostructures for signal enhancement will be discussed. Secondly, we will illustrate recent advances for indirect diagnosis using active nanomaterials, Raman reporters, and specific capture elements as SERS tags. Thirdly, critical challenges for translating the potential of the SERS sensing techniques into clinical applications via machine learning and portable instrumentation will be described. The unique nature and integrated sensing capabilities of SERS provide great promise for early cancer diagnosis or fast pathogens detection, reducing sanitary costs but most importantly allowing disease prevention and decreasing mortality rates.

**Keywords:** Nanotechnology, Cancer and pathogens, Medical diagnosis, SERS, Plasmonic metal, Nano-hybrid, Magnetic materials, SERS tags

## Background

One of the biggest challenges of healthcare systems worldwide is the fast diagnosis of issues such as cancer and pathogens [1]. Early diagnosis can help decrease overall costs in treating such issues and most importantly, decrease the mortality rates. Yet, target biomarkers are present at extremely low levels in early cancer stages [2]. Pathogens can be grown *in-vitro* to obtain sufficient cells, increasing the detection sensitivity, yet such procedures are time-consuming. The balancing between fast

discrimination and sensitive detection of pathogens is the key to providing effective guidance in antibiotic therapy [3, 4]. In addition, disease diagnosis is also hampered by the inherent complexity of biological media, which prevents direct detection without sample processing [5, 6].

SERS is a very promising tool for the direct detection of biomarkers in disease diagnosis applications. The technique relies on the enhancement of inelastic light scattering molecules (or analytes) attached or combined with plasmonic metals or semiconductor materials [7–9]. Since the first discovery of the SERS in 1974, researchers have proven its suitability in analytical science, ranging from environmental monitoring to biological/biomedical detection [10–14]. The broad scope of operations and applications, along with the high sensitivity, rich

\*Correspondence: beatrizjurado@uah.es; alberto.escarpa@uah.es

<sup>2</sup> Department of Analytical Chemistry, Physical Chemistry, and Chemical Engineering, University of Alcalá, Alcalá de Henares, 28802 Madrid, Spain  
Full list of author information is available at the end of the article

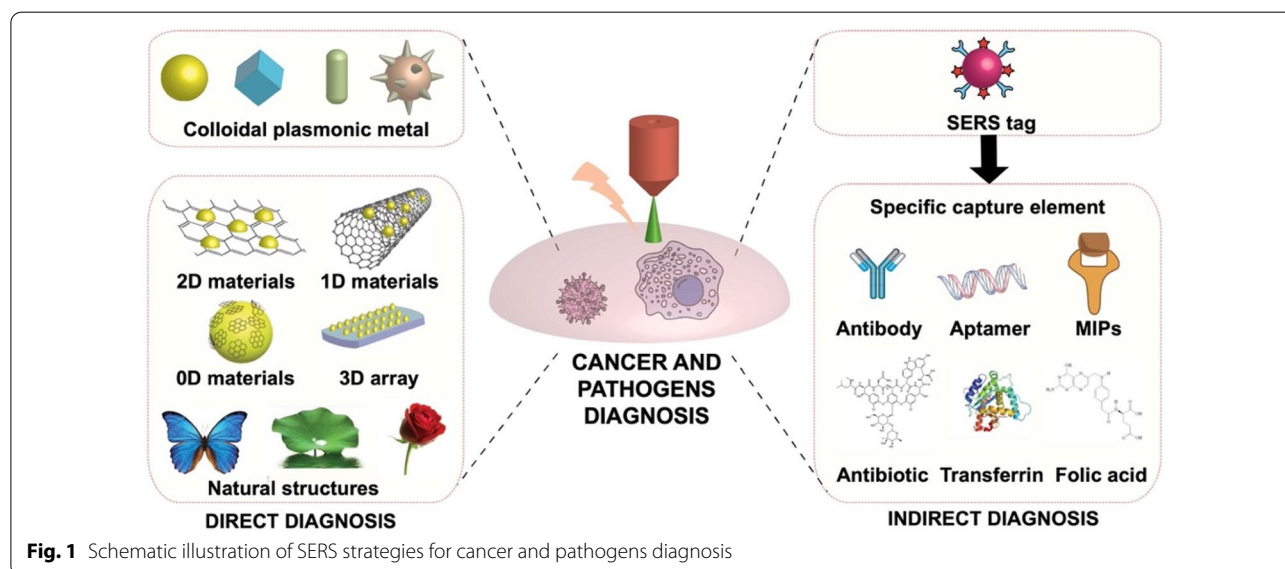


© The Author(s) 2022. **Open Access** This article is licensed under a Creative Commons Attribution 4.0 International License, which permits use, sharing, adaptation, distribution and reproduction in any medium or format, as long as you give appropriate credit to the original author(s) and the source, provide a link to the Creative Commons licence, and indicate if changes were made. The images or other third party material in this article are included in the article's Creative Commons licence, unless indicated otherwise in a credit line to the material. If material is not included in the article's Creative Commons licence and your intended use is not permitted by statutory regulation or exceeds the permitted use, you will need to obtain permission directly from the copyright holder. To view a copy of this licence, visit <http://creativecommons.org/licenses/by/4.0/>. The Creative Commons Public Domain Dedication waiver (<http://creativecommons.org/publicdomain/zero/1.0/>) applies to the data made available in this article, unless otherwise stated in a credit line to the data.

molecular “finger-print” information (specificity), in-situ detection, and non-destructive nature [15–17], have paved new ways for SERS application in cancer and pathogens diagnosis [18, 19]. Indeed, cancer and pathogenic cells and related biomarkers are mostly composed of proteins or other organic molecules with inherent Raman signals, allowing for direct detection and target discrimination based on the different Raman responses (*finger-prints*) of their compositions. Other key features of SERS include high sensitivity and fast detection, allowing disease diagnosis even at a signal cell/molecular level [20–22]. The type, size, and shape of the SERS substrate used for enhancing the Raman signal will exert a strong influence on a given biological application. This is of extreme importance to also address the critical challenge of non-specific interactions with co-existing substances in the biological matrices, which can hamper sensitivity. SERS substrates can be classified into two main groups according to the enhancement mechanism: (a) electromagnetic enhancement (EM) or (b) chemical enhancement (CM). EM derives its enhancing ability from electromagnetic effects on nano-structured metallic surfaces, reaching an enhancement factor (EF) of  $10^4$ – $10^{10}$ . CM is caused by charge transfer, with a lower degree of the overall Raman enhancement (2 orders) [23, 24]. The integration of both mechanisms into hybrid SERS substrates shows considerable promise for synergetic enhancement and metal protection, achieving fast and reliable disease diagnosis in biological samples, and avoiding interferences in most cases [25, 26]. Using ingenious designs such as magnetic separation or introducing SERS tags labeled with recognition elements, the disease diagnosis can be conducted with high selectivity [27, 28]. Figure 1 illustrates

a schematic summary of the previously described strategies.

As can be seen in Fig. 1, the main advantage of SERS in cancer and infectious diseases diagnosis is the ability for the direct and fast detection of the cells or related biomarkers by exploiting the specific Raman fingerprint in discrimination, which originates from the different Raman-active molecules of the cell lines [29–32]. Indeed, disease diagnosis conducted in this way can provide a rich spectrum containing information about the analyte, allowing for further in-depth studying of related diseases at the molecular level [33–35]. The major challenge of current direct detection is the low content and small Raman scattering cross-section of Raman active chemicals on the cell surface, leading to weak SERS signals and limited sensitivity in disease diagnosis [36, 37]. Therefore, different substrates for signal enhancement have been explored [38]. Colloid plasmonic metals with EM effect such as gold and silver nanoparticles have been the traditional choices [39, 40]. To increase the efficiency of the Raman enhancement, nanomaterials of different shapes such as nanostar, nanorod, nanocube, etc., with abundant branches or edges, were explored [41–43]. In addition, semiconductors with CM effect, such as graphene,  $\text{MoS}_2$ , etc., have been also introduced to further improve SERS properties [44–46], as well as for protecting active tags from degradation, or to impart further surface functionalities [47, 48]. Apart from sensitivity, signal stability is another challenge in the direct diagnosis of cancer and pathogens. Colloidal SERS substrates prepared by simply mixing the tag with the biological sample are prone to the generation of heterogeneous and random *hot-spots*, which leads to differences in enhancement factors to the



Raman active molecules and unstable signals [12, 49, 50]. 3D-ordered SERS substrates are a convenient alternative to avoid such problems [51–54]. Natural creatures possess ordered nanostructures, endowing them with specific functionalities such as hydrophobicity, strong adhesive force, etc. [55–57]. Such natural nanostructures also are widely used in fabricating low-cost 3D solid substrates for SERS [58, 59]. In addition, cancer and pathogens diagnosis using SERS is hampered by interferences from the complex biological matrix used, which is also a critical point in clinical application. A typical solution relies on the introduction of an indirect SERS strategy, involving a Raman reporter, SERS active nanomaterial, and specific recognition element to fabricate a “three-in-one” SERS tag, thus providing a strong SERS signal, and realizing specific affinity with target cells even in a complex matrix [60–62].

In this review, we will describe recent advances and prospects in SERS-based approaches for cancer and pathogens diagnosis. As a distinct point, this review will cover both cancer and pathogens diagnosis, and most importantly, will focus on different strategies to improve SERS performance in a view to providing the readers with important tools to improve overall credibility and analytical performance with diagnosis purposes. We will discuss first direct SERS strategies for sensing cancer and pathogens cells and related biomarkers, including the design of different SERS substrates such as plasmonic, semiconductor structures, and 3D order nanostructures for signal enhancement. Secondly, we will illustrate recent advances for the indirect diagnosis of cancer and pathogens by the introduction of SERS tags, which combine SERS active nanomaterials, Raman reporters, and specific capture elements into “three-in-one” probe units. Thirdly we will be, for the first time, a critical overview of challenges and solutions to translate the existing proof-of-concept applications into real clinical settings, covering from portable SERS detection to machine learning to discriminate the rich but complex SERS spectra. Further challenges will be briefly discussed in the conclusions. The unique nature and integrated sensing capabilities of SERS provide great promise for early cancer diagnosis or fast pathogen detection, reducing sanitary costs but most importantly allowing disease prevention and decreasing mortality rates.

### Direct SERS detection of cancer and pathogens

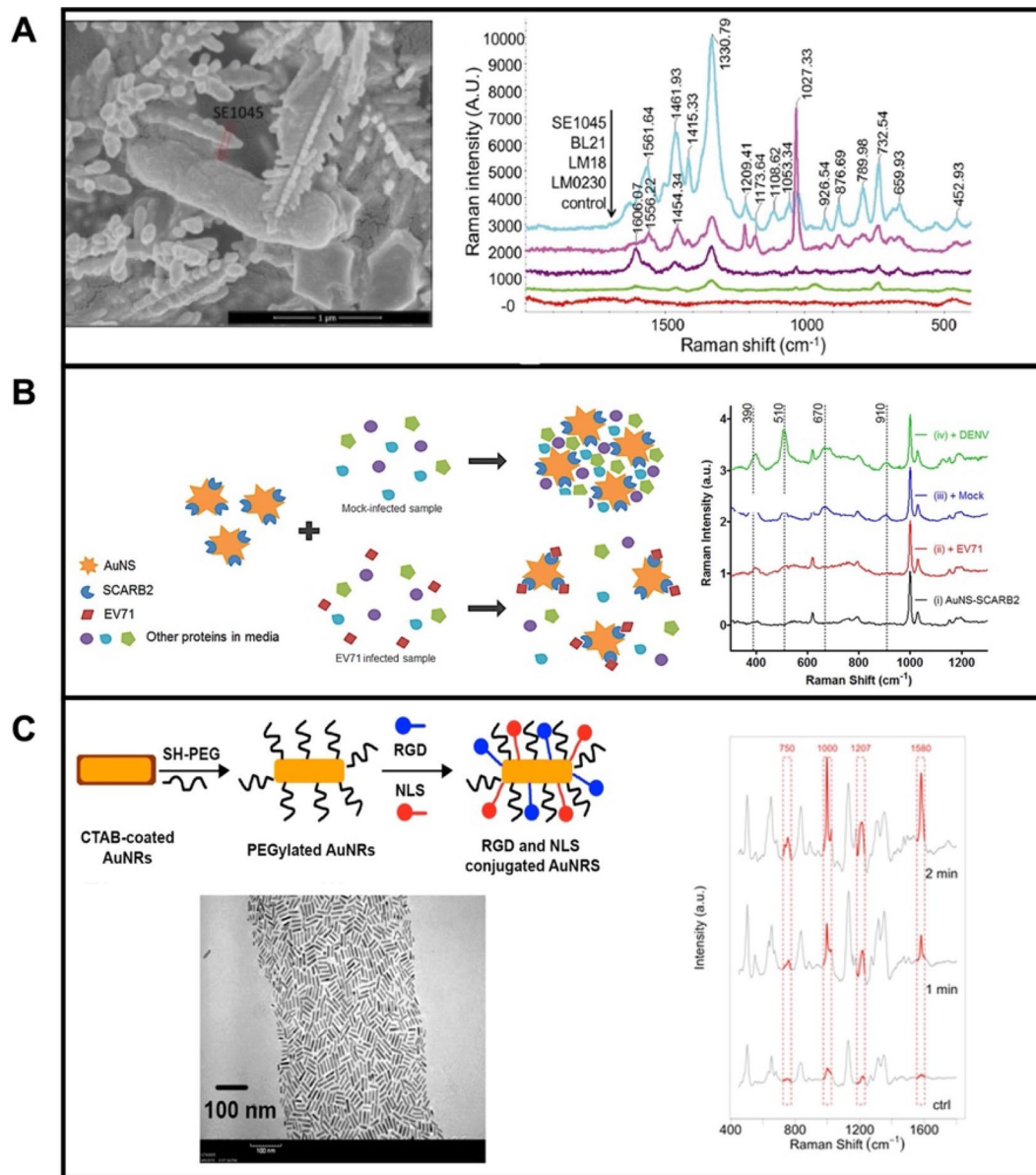
Direct SERS sensing of target analytes is achieved by direct attachment to the SERS substrate, obtaining both qualitative (“finger-print” of spectra) and quantitative (signal intensity) determination [63]. A major superiority of direct SERS over other strategies is the obtention of a rich spectrum with “finger-printing” information of

the target molecules without the need for further labeling [64–66]. In the diagnosis of cancer and pathogens, this strategy can provide in-depth information from biomarkers, cells, and/or their interactions, thus providing the possibility for revealing target compositions and disease mechanisms [67–70]. Yet, the low content of Raman active molecules on the cell surfaces, the low concentrations of related biomarkers, and the complexity of biological fluids, results in low signal intensities, hampering this detection. In addition, the heterogeneous aggregation of the SERS active nanoparticles can lead to low reproducibility. The key to achieving high sensitivity and reproducibility is to select and tailor the composition of the SERS substrates.

### Plasmonic metal nanoparticles as SERS substrates

Direct SERS sensing with i.e., silver, gold, and copper nano colloids involves the direct mixing with the sample to induce the generation of biomarker-nanoparticle or cell-nanoparticles aggregates. The as-generated SERS spots will increase the intensity of the Raman signal. Different metal nanomaterials with variable shapes have been explored, including nanoparticles [71, 72], nanorods (NRs) [73, 74], nanostars [75, 76], nanocubes [77, 78], etc. For example, Wang et al. [79] synthesized silver dendrites for direct SERS detection and discrimination of *Salmonella enterica* in the presence of *Escherichia coli* (see Fig. 2A). Thus, the scanning electron microscopy (SEM) images show the morphology of the silver dendrites-*Salmonella enterica* complex (left part). Further mapping of the specific peaks allows for the specific detection (Raman shift,  $1332\text{ cm}^{-1}$ ) of *Salmonella enterica* with a limit of detection (LOD) of  $10^4\text{ CFU mL}^{-1}$  (see middle part). In addition, such SERS substrates have higher enhancement activity for Gram-negative bacteria than for Gram-positive bacteria, avoiding thus interferences for selective discrimination (right part).

Reyes et al. [80], developed a SERS strategy for direct and rapid determination of Enterovirus 71 (EV71) using Au nanostars colloids as plasmonic substrates (Fig. 2B). The surfaces of Au nanostars were modified with EV71 affinity protein, and recombinant scavenger receptor class B member 2 (SCARB2) protein, for the further specific detection of the target. Nonspecific proteins from the sample would induce the aggregation of SCARB2-modified Au nanostars, producing Raman signals (peaks at 390, 510, 670, and  $910\text{ cm}^{-1}$ ). While EV71 viruses are presented in the biological sample, SCARB2-modified Au nanostars can be combined with EV71, followed by the anti-aggregating of Au nanostar colloids and the diminishing of the Raman peaks (left part). Figure 2B revealed that peaks at 510, 670, and  $910\text{ cm}^{-1}$  only disappear in the presence of EV71 virus while not in the



**Fig. 2** **A** Direct SERS sensing of bacteria using Ag dendrites as Raman substrates: SEM images of the *Salmonella enterica* (SE1045) mixed with Ag dendrites (left) and SERS spectra of different bacteria strains using Ag dendrites as substrate. **B** Gold nanostars as SERS substrate for direct diagnosis of enterovirus (EV) 71: schematic of EV71 SERS sensing based on anti-aggregation of gold nanostars and Raman spectra of SCARB2 modified Au nanostars added to mock-infected cell culture in the presence and absence of EV71 and the presence of DENV. **C** Gold nanorod as SERS substrates for studying cancer cell death mechanisms: schematic of the sensing strategy, TEM images of the modified nanorods, and SERS spectra collected of a single HSC-3 cell under NIR laser exposure for 1 and 2 min. Reprinted with permission from ref. [79] (A); [80] (B) and [87] (C)

presence of Dengue virus (DENV) or mock-infected cell culture supernatants, which proved the high specificity of the proposed method.

Plasmonic nano colloids such as Au nanorods (AuNRs) [81, 82], multilayered Au nanoshells [83], Au nanostars [84], etc., not only show excellent SERS activity but also highly efficient photothermal

conversion upon near-infrared (NIR) irradiation, thus have been used in cancer-related photothermal therapy. The *in-situ* detection and time-dependent changes of Raman fingerprints of target molecules in such substrates are also advantageous to explore the mechanism of cancer-related biological and chemical processes [85, 86]. Ali et al. [87] employed AuNRs

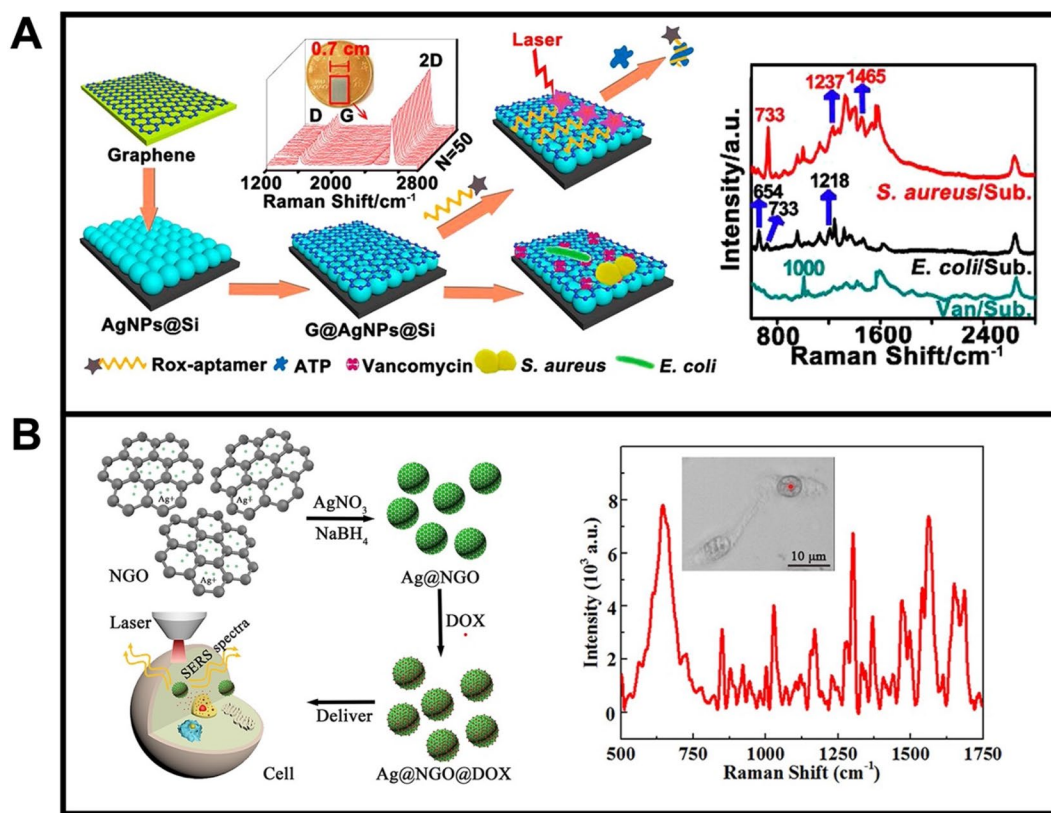
with high photothermal conversion efficiency to study its underlying photothermal effect (Fig. 2C). Using a seedless method, AuNRs with average sizes of 25 nm × 6 nm were obtained. Further surface modification of PEG, Arg-Gly-Asp (RGD), and nuclear localization signal (NLS) improve the biocompatibility, cell uptake, and targeting ability of the AuNRs (Fig. 2C). After cell (HSC-3 cell) uptake, a NIR laser was used to irradiate the cells at different time intervals, leading thus to an increase in the temperature. Simultaneously, the Raman spectra were recorded to monitor molecular changes from the AuNRs containing microenvironment. As depicted in Fig. 2C, peak intensities at 750, 1000, 1207, and 1580 cm<sup>-1</sup> increased after exposure to the NIR laser. From the changes in SERS peaks, the authors deduced related conclusions including “phenylalanine increases in the microenvironment (perturbation of phenylalanine metabolism) during photothermal therapy,” and “apoptotic cells” (*cytochrome c*-mediated apoptosis) increase during thermal heating.” Combined with metabolomics and proteomics experiments, this work demonstrates the potential of AuNRs for photothermal therapy at and from the molecular level. Other plasmonic colloid metals used as SERS substrates for direct sensing of cancer, pathogens, and related biomarkers are summarized in Table 1.

### Nanomaterials incorporated plasmonic metal nano-hybrids as SERS substrates 2D nanomaterials

The convenient marriage of plasmonic metal and 2D nanosheets led to novel platforms with high SERS activity, high stability, low background signal, and multi-functionality with a broad scope of applications [97–100]. Meng et al. [101] developed a graphene-silver nanoparticles-silicon (G@AgNPs@Si) sandwich SERS chip, as depicted in Fig. 3A. AgNPs were grown in situ on silicon substrates (Si), followed by wrapping Ag surfaces with graphene (G) monolayer. Such G@AgNPs@Si nano-hybrids show synergistic effects including electromagnetic enhancement (Si-reflected plasmon resonance; AgNPs-scattered plasmon resonance) and chemical enhancement (graphene-based charge-transfer resonance), which results in superior SERS activity. The chip was modified with vancomycin for direct capture and sensing of *Staphylococcus Aureus* and *Escherichia Coli*. Figure 3A shows the representative Raman peaks of *Staphylococcus Aureus* (1237 cm<sup>-1</sup> and 1465 cm<sup>-1</sup>) and *Escherichia Coli* (654 cm<sup>-1</sup> and 1218 cm<sup>-1</sup>) bacteria, illustrating the selectivity of the protocol. Zeng et al. [99] fabricated a SERS substrate using nanosized graphene oxide coated with silver nanoparticles (Ag@NGO). The NGO showed superior chemical inertness and optical penetration (Fig. 3B), along with a uniform size (~20 nm diameter) and round morphology, to facilitate

**Table 1** Plasmonic colloid metal as SERS substrate for direct sensing of cancer, pathogens, and related biomarkers

Target analyte/cell	Interaction mode	Peaks (cm <sup>-1</sup> )	Sensitivity	Refs.
Ag NPs				
<i>Staphylococcus aureus</i>	Aptamer as capture elements	735, 1337, 1458	1.5 CFU mL <sup>-1</sup>	[88]
Prostatic cancer (DNA/RNA) biomarkers	Electrostatic interaction	560, 742, 788, 913, 1035, 1180, 1247, 1334, 1457, 1539, 1632	100 copies of input RNA	[89]
<i>Mycobacterium bovis BCG</i> , <i>Mycobacterium tuberculosis</i> , <i>Staphylococcus aureus</i> , <i>Staphylococcus epidermidis</i> , <i>Bacillus cereus</i>	In-situ coating	731, 1031, 1326, 1463	10 <sup>2</sup> CFU mL <sup>-1</sup>	[90]
Prostate cancer (RNA) biomarkers	Electrostatic interaction	742	100 synthetic RNA copies	[91]
AuNPs				
Colorectal cancer biomarkers	–	724, 1263, 1574	Above 90%	[92]
Au nanostars				
Protein Kinase A activity for cancer screening	–	725, 1395	–	[93]
Au/Ag bimetallic NPs				
<i>Escherichia Coli</i> , <i>Salmonella typhimurium</i> , <i>Bacillus subtilis</i>	–	656, 730, 958, 1082, 1324, 1581	–	[94]
Core-shell Au@Ag NPs				
<i>Escherichia coli</i> , <i>Staphylococcus aureus</i>	Interaction between negative (bacteria) and positive (PEI)	655, 729, 958, 1328, 1583 ( <i>E. coli</i> ) 733	10 <sup>3</sup> CFU mL <sup>-1</sup>	[95]
Exosomes as cancer biomarkers	Electrostatic attachment and in situ formation	668, 707, 786, 1179, 1490, 1563 (B16F10) 645, 1000, 1211, 1326, 1381, 1563, 1592 (RBC) (RBD)	> 90%	[96]



**Fig. 3** **A** Graphene-silver nanoparticles-silicon (G@AgNPs@Si) as SERS substrate for bacteria discrimination: Schematic illustration of the strategy and corresponding SERS spectra for *Staphylococcus Aureus* and *Escherichia coli*. **B** Nanosized graphene oxide coated with silver nanoparticles (Ag@NGO) as SERS substrate for intracellular detection: schematic illustration of the synthesis and corresponding intracellular SERS biosensing and SERS spectrum of HepG-2 after incubation with Ag@NGO nano-hybrid (right). Reprinted with permission from ref. [101] (A) and [99] (B)

intracellular uptake in further biomedical sensing applications (middle). Specific peaks such as 1651, 1564, 1302, 1030, 850, and 642 cm<sup>-1</sup> are obtained in the SERS spectra of HepG-2 cancer cells (right). Such Raman signals are only produced inside the cells, indicating the successful cell penetration of the Ag@NGO nanoparticles.

An updated list of recent 2D nanomaterials such as BP, g-C<sub>3</sub>N<sub>4</sub>, MoS<sub>2</sub>, h-BN, and WS<sub>2</sub> used in connection with plasmonic metals as SERS substrates for cancer and pathogens diagnosis are listed in Table 2.

### 1D nanomaterials

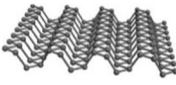
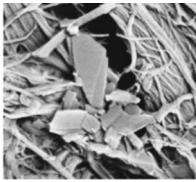
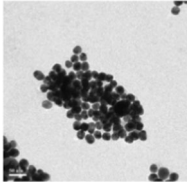
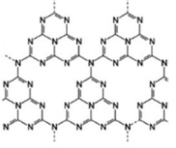
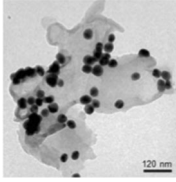
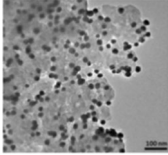
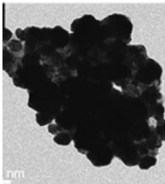
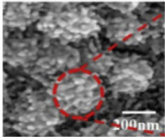
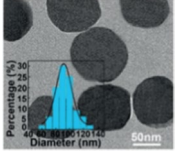
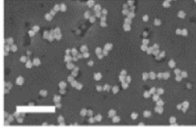
As an important member of the 1D materials family, carbon nanotubes (CNTs) have broad applications ranging from extraction and enrichment to biological sensing due to their unique structure and properties [111–113]. CNTs comprise single-wall carbon nanotubes (SWCNTs) and multi-wall carbon nanotubes (MWCNTs), which are composed of sp<sup>2</sup>-hybridized carbon atoms, exhibiting high chemical stability [114], large surface area [115] and biocompatibility [116]. The inherent tubular morphology of CNTs allows for the direct growth of plasmonic metal

on their surfaces without any pretreatment. In addition, the as-deposited nanoparticles are restricted to the nanoscale size due to the small diameter of CNTs [117]. Researchers have also exploited the inherent stability of SWCNTs against photo-bleaching to design a myriad of radiometric SERS nanosensors [118, 119]. The use of CNTs-based hybrid as SERS substrates has been successfully illustrated for the direct detection of explosives and other toxic molecules [120, 121], yet applications for detection in the biomedical field remain unexplored.


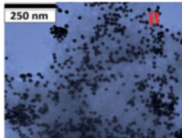
### 0D nanomaterials

Compared to traditional 2D nanosheets, 0D materials show unique advantages, such as higher adsorption abilities due to the larger specific surface areas [122] or higher SERS activity derived from Van Hove singularities in the density of states [123]. Bhunia et al. [124] reported the development of carbon-dot/silver-nanoparticle (C-dot-Ag-NP) PDMS SERS films for bacteria sensing. For preparation, the PDMS precursors and ascorbic acid are heated at 60°C to form the PDMS film. The encapsulated ascorbic acid function as a carbon precursor for C-dot

**Table 2** 2D materials plasmonic metal as SERS substrate

2D nanomaterial	Nano-hybrid	Hybrid structure	Target analyte/cell	Refs.
 <p>Black phosphorus (BP)</p>	BP-Au filter		<i>Staphylococcus aureus</i> <i>Escherichia coli</i> <i>Listeria</i>	[102]
	BP-Au nanosheets		HepG2 cells	[103]
$g-C_3N_4$ 	$g-C_3N_4$ nanosheet Au@Ag	 120 nm	Breast tumors Fibroblasts HeLa cell	[104] [105] [106]
	Mesoporous $g-C_3N_4$	 200 nm	6-thioguanine	[107]
	MoS <sub>2</sub>	MoS <sub>2</sub> -Au nanosheets	 20 nm	Fibroblasts
	AuNPs/GO@MoS <sub>2</sub> /AuNPs	 200 nm	DNA	[108]
Boron nitride (BN)	Cu@HG@BN nanosheets	 50 nm	In vitro microRNA sensing	[109]
	AuNS@hBN		Quorum sensing of bacterial biofilms	[69]

**Table 2** (continued)

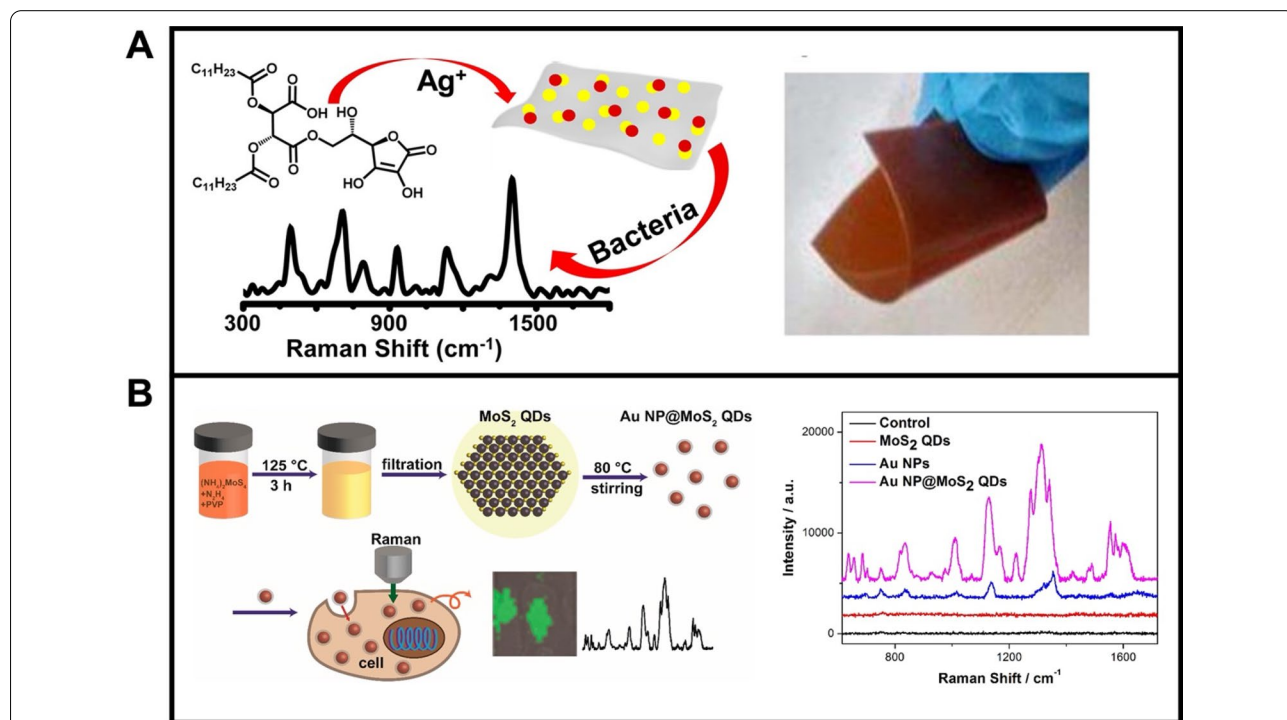
2D nanomaterial	Nano-hybrid	Hybrid structure	Target analyte/cell	Refs.
 WS <sub>2</sub>	WS <sub>2</sub> -Au nanosheets		<i>Salmonella DT104 Salmonella Typhi</i>	[110]

formation by reduction with silver acetate at 125 °C (Fig. 4A). Such design results in the generation of uniform C-dots with diameters between 2 and 5 nm, along with flexible nature. The integration of AgNPs and C-dots played a critical role in the high SERS activity, whereas no Raman peaks were obtained using PDMS films containing only AgNPs or C-dots. The C-dot-Ag-NP-PDMS films were applied for the detection of *Pseudomonas Aeruginosa*, as well as distinguishing between *Bacillus Aureus*, and *Erwinia Amylovora* 238 bacteria. Fei et al. [125] employed Au NPs@MoS<sub>2</sub> quantum dots (Au NP@MoS<sub>2</sub> QDs) nano-hybrids as SERS substrates for cancer cell imaging (Fig. 4). As indicated in the TEM observation, such nano-hybrid possess core-shell structures with

an ultrathin MoS<sub>2</sub> QDs-coating. Such AuNPs@MoS<sub>2</sub> QDs nano-hybrids were further used for 4T1 cell imaging, which showed much higher SERS intensity compared with single MoS<sub>2</sub> QDs or AuNPs.

**3D-ordered solid nanostructures as SERS substrates**

One obstacle that traditional plasmonic nanoparticle-based SERS sensing is the need to overcome the low repeatability of the signal intensity. Thus, the aggregation of the nanoparticle colloids is random and heterogeneous, resulting in different SERS enhancement abilities to the attached target analytes even in the same sample [126, 127]. 3D solid nanostructures hold great promise to solve this drawback. Indeed, the composition of 3D



**Fig. 4** **A** Carbon-Dot/Silver nano-hybrid as SERS films for bacteria detection: schematic illustration of the synthesis of C-dot-Ag-NP-PDMS films, photography showing the flexibility of the film and SERS spectrum of 10<sup>4</sup> CFU/mL of *Pseudomonas Aeruginosa* **B** AuNP@MoS<sub>2</sub> quantum dots nano-hybrid for SERS sensing of cancer cells: schematic illustration of the synthesis of AuNP@MoS<sub>2</sub> quantum dots nano-hybrid and related biological SERS application and SERS spectra of 4T1 cells mixed with MoS<sub>2</sub> QDs (red line), AuNPs (blue line) and AuNP@MoS<sub>2</sub> nano-hybrid (violet line). Reprinted with permission from ref. [124] (A) and [125] (B)



nanostructures can be tailored to obtain periodic nanostructures with specific nanogaps at fixed positions, resulting in good repeatability and sensitivity to SERS sensing [12, 128, 129]. The synthesis is conducted by bottom-up self-assembly methods [130, 131] or top-down nanolithography techniques [132, 133]. Nanosphere lithography (NSL) is a widely used approach to synthesized 3D surfaces. NSL consisted of the formation of a monolayer of nanospheres with uniform sizes on a flat surface, followed by the deposition of a noble metal film using thermal evaporation or electron beam deposition. Next, a sonication or stripping process is used to remove the resulting hybrid nanospheres [134–136]. Electron beam lithography (EBL) is widely used for top-down fabrication of periodic nanostructures with arbitrary shapes and tunable interparticle nano-gaps in a small distance, which is key for both repeatability and high active SERS enhancement [137, 138]. 3D nanostructures with specific designs have been used as SERS substrates for cancer and pathogens detection, including Ag arrays, Ag nanoring cavities, Au octupolar meta structures, etc. Typical examples are listed in Table 3.

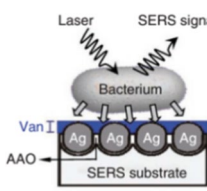
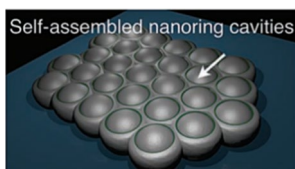
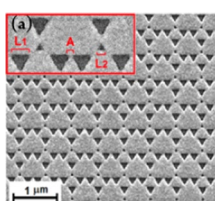
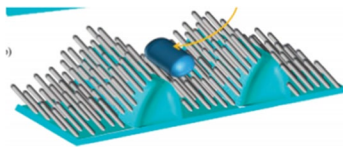
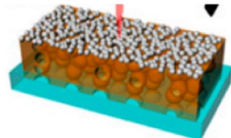
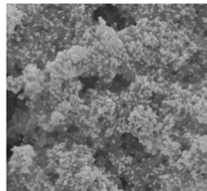
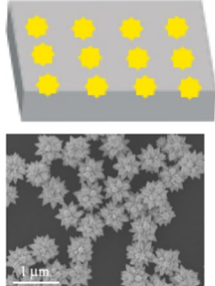
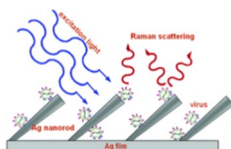
Natural structures have been explored for the preparation of 3D surfaces, further evaluating the potential for SERS sensing. For instance, hierarchical nanostructures impart lotus leaf and rose petals with surface superhydrophobicity [151, 152], photonic crystals are present in butterfly wings [153], and the high density of nano-size tentacles in toepads make gecko exhibit strong adhesive force to the wall [154], etc. Such natural periodic 3D structures can function as excellent bio-templates for decoration with noble metal NPs to fabricate SERS substrates [59, 155, 156]. Shao et al. [157] used cicada wings as bio scaffold arrays for decoration with AgNPs, forming thus 3D SERS substrates with hierarchical nanogaps. As depicted in Fig. 5A, the decoration of the bio-template is conducted by ion-sputtering techniques. SEM observation illustrates the periodic 3D nanostructure, resulting in a high reproducibility in target sensing, along with nanogaps to generate more hot spots for sensitive detection. Lateral real application has used this bio-SERS substrate for the discrimination among PCV2, PRV, and H5N1 viruses due to the specific Raman spectrum and discrimination analysis. Tan et al. [158] exploited the photonic crystals of butterfly wings as bio-templates for modification with Cu superstructures (Fig. 5B). However, the original chitin and protein from butterfly wings caused SERS signal impurities and fluorescence interferences in target sense. To solve such an issue, the authors employed a reduction method using H<sub>2</sub> to obtain Cu decorated wing SERS substrate with low background signals. The SEM images of Fig. 5B show the morphology of the biotemplate after the reduction process, with no obvious

changes in the morphology after reduction by H<sub>2</sub> in elevated temperature. Compared with unmodified butterfly wings, Cu butterfly wings showed clean SERS spectra after the reduction process, with adequate adenine and guanine (DNA) detection, with excellent sensitivity at a low cost.

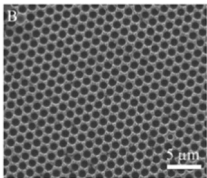
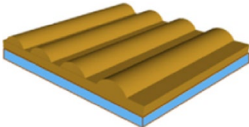
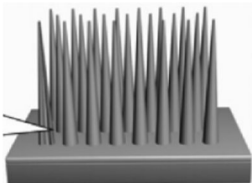
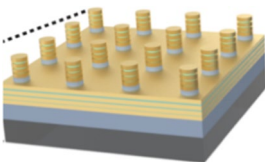
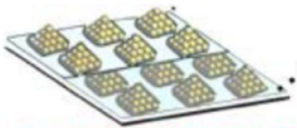
### Magnetic SERS substrates

The use of magnetic actuated SERS substrates is beneficial for SERS sensing due to the facilities for simultaneous target capture and separation, interferences removal, and centrifugation avoiding thus interferences, especially from biological samples. The most widely used structures compromise a magnetic core and a metallic shell. Diverse types of magnetic materials have been used, including Fe<sub>3</sub>O<sub>4</sub> [159, 160], MnFe<sub>2</sub>O<sub>4</sub> [161], CoFe<sub>2</sub>O<sub>4</sub> [162], Ni [163, 164], FePt [165] or CoPt [166]. The coating of the magnetic core with plasmonic nanoparticles can be performed by in-situ growth [167, 168] or ex-situ assembly [169, 170] methods. For example, Wang et al. [171] synthesized Fe<sub>3</sub>O<sub>4</sub>@SiO<sub>2</sub>@Ag nano-hybrid with a flower-like shape for capturing and sensing bacteria. As shown in Fig. 6A, SiO<sub>2</sub> beads are coated with magnetic nanoparticles, followed by silver grown on their surfaces. Interestingly, by adjusting the amount of AgNO<sub>3</sub>, the structure of the nano-hybrid can be tailored into a micro-flower shape with a high degree of branches. Such design endows the nano-hybrid with superiorities: (a) excellent dispersion for improved response to the applied magnetic field; (b) larger surface area for enhanced target capture; (c) sharp tips from the branches for better hot spots in Raman signal enhancement; and (d) the possibility of sample preconcentration due to the presence of a magnetic Fe<sub>3</sub>O<sub>4</sub> core. The resulting Fe<sub>3</sub>O<sub>4</sub>@SiO<sub>2</sub>@Ag nano-hybrid was modified with an aptamer for specific capture of *Staphylococcus Aureus* (Fig. 6A), with a limit of detection of 10<sup>4</sup> cells per milliliter. In another example, Fe<sub>3</sub>O<sub>4</sub>@Au nano-hybrids were prepared by ex-situ assembly of 3 nm of AuNPs seed into Fe<sub>3</sub>O<sub>4</sub> (Fig. 6B) [95]. By further coating the Fe<sub>3</sub>O<sub>4</sub>@Au with positive polyethyleneimine (PEI), the nano-hybrid can capture negative bacteria by electrostatic interactions, allowing for the capture and SERS-enhanced detection of *Escherichia Coli* and *Staphylococcus Aureus* bacteria. Related SEM measurements showed that Au surfaces of the nano-hybrid were attached to the bacterial wall, generating a Fe<sub>3</sub>O<sub>4</sub>@Au@PEI-bacteria complex. With the enrichment effect of the magnetic core and SERS activity outer Au surface, the LOD is 10<sup>3</sup> cells per mL. The different Raman fingerprinting of the analytes can be subjected to principal component analysis (PCA) for the discrimination among bacteria. (Fig. 6B).

**Table 3** 3D ordered nanomaterials as SERS substrates for direct sensing of cancer, pathogens, and related biomarkers

Nanomaterial	Schematic of the SERS substrate	Target analyte/cell	Interaction mode	Refs.
AgNPs arrays		<i>Lactobacillus plantarum</i> , <i>Escherichia coli</i>	Vancomycin as capture element	[139]
Ag nanoring cavities		DNA base (adenine)	Direct contact	[140]
Au octupolar metastructures		<i>Brucella</i>	Phage as capture elements	[141]
Silver nanorod (AgNR) array on PDMS substrate		<i>Pseudomonas aeruginosa</i>	Direct contact	[142]
AgNPs on a mesoporous silicon substrate		<i>Escherichia Coli</i> <i>Staphylococcus Epidermidis</i>	Direct contact	[143]
Ag film substrate		Circulating tumor cells (CTCs)	Direct contact	[144]
Highly branched AuNPs on a silicon wafer		Carcinoma cancer cells	Direct contact	[35]
Ag nanorod array		Respiratory viruses (RSV) strains A2, A/Long, and B1	Direct contact	[145]

**Table 3** (continued)

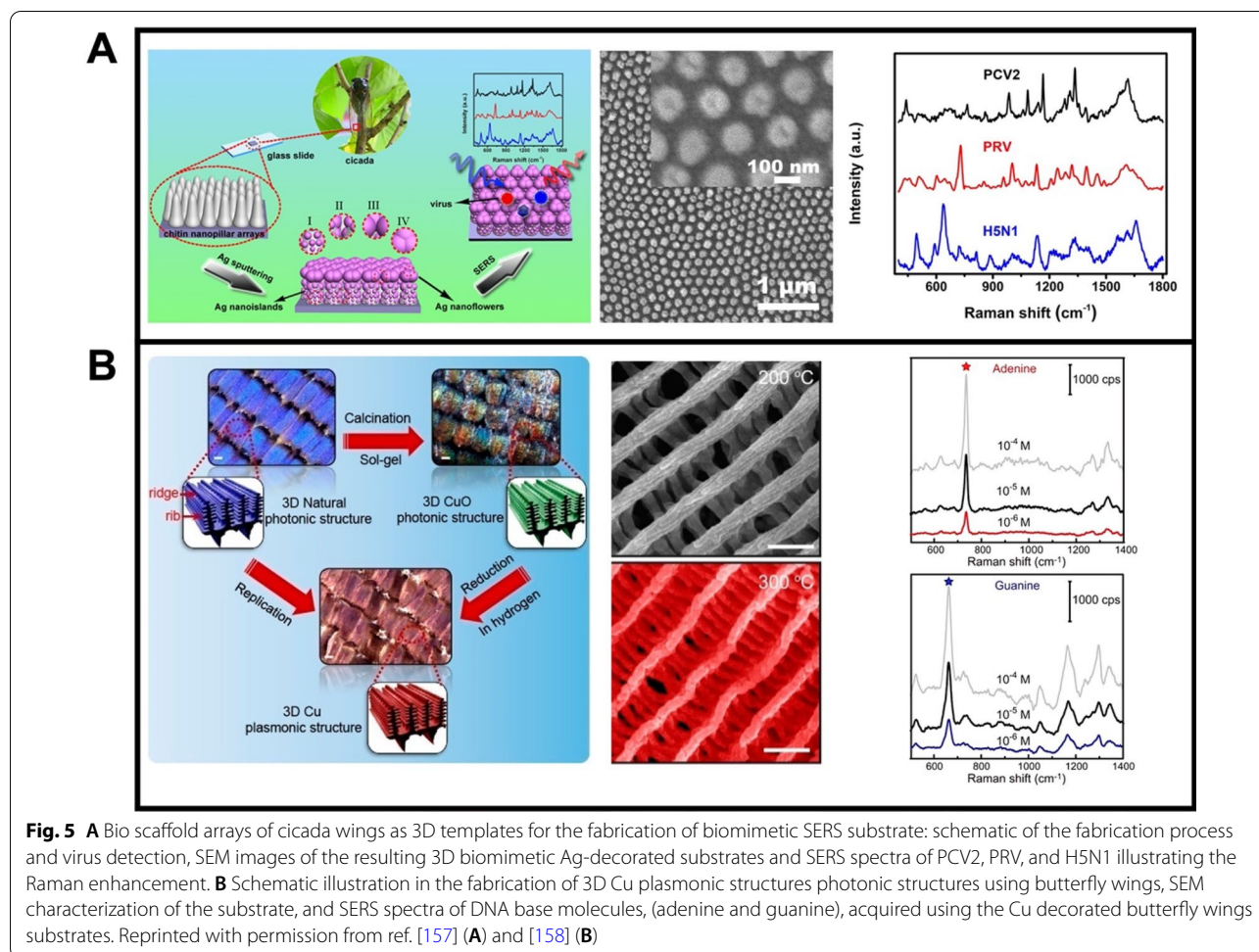
Nanomaterial	Schematic of the SERS substrate	Target analyte/cell	Interaction mode	Refs.
Ag-Cr coated nanovoid structure		Cytochrome C	Direct contact	[146]
Au grating		DNA (discriminated DNA-DNA interaction)	Complementary between single oligonucleotide	[147]
Ag-coated nanowire arrays		<i>Bacillus anthracis</i> spores	Direct contact	[148]
Multilayered metal-insulator-metal nanostructures		Breast cancer	Grown on the substrate directly	[149]
Au ordered superlattices		Kynurenine, tryptophan, and purine derivatives	Direct contact	[150]

Yang et al. [172] used  $\text{Fe}_3\text{O}_4/\text{Au}/\text{Ag}$  nano-hybrids for adenosine sensing in a urine sample from lung cancer patients. To avoid interference from urea, an azo coupling reagent was employed to eliminate the urea (Fig. 6C). Such design allows for the fast determination of trace cancer biomarkers (adenosine) directly from urine samples (Fig. 6C).

#### Non-plasmonic nanostructures as SERS substrates

Raman signal enhancement mechanisms based on EM enhancement employ plasmonic noble metals as SERS substrates [173, 174]. Semiconductor materials -either organic or inorganic- possess inherent Raman signals enhancement by charge-transfer mechanisms, paving a new way for SERS based on CM [175]. Advantages of the use of such nanomaterials include chemical stability, resistance to degradation, high absorptivity, and low cost [176–179]. Such properties endow the semiconductor-based SERS substrate with promising applications in cancer and pathogens cells or biomarker sensing. Inorganic semiconductors are based on solid-state structures of metal oxides [180, 181], metal sulfides [182, 183], metal

halides [184, 185], and single elements [186, 187]. Hal-davnekar et al. [188] fabricated ZnO-based semiconductor quantum probes for cancer cell's SERS sensing. After performing femtosecond laser interaction, the size of the ZnO semiconductor was reduced to quantum scale (Fig. 7A), which is key to getting a high SERS activity with an enhancement factor of up to  $\sim 10^6$ . The quantum scale semiconductors were combined with 3D nano-dendrite platforms for self-targeting, cell adhesion, and proliferation. The proposed platform was utilized for in-vitro sensing of two cancer cell lines. As depicted in the SEM images of Fig. 7A, Hela cells, breast cancer (MDAMB231) cells, and fibroblast (NIH3T3) can adhere to the nano-dendrite platform. The corresponding SERS spectra also showed distinct fingerprints for each type of cell. Keshavarz et al. [189] used multiphoton ionization growth on a Ti substrate, to fabricate  $\text{TiO}_x$  (Q-structured) nano particles restricted to the quantum scale (Fig. 7B). The resulting  $\text{TiO}_x$  semiconductors display high SERS activity with an enhancement factor of  $3.4 \times 10^7$ . Figure 7B (right) shown the SEM morphology of fibroblast-NIH3T3 cell (i), Hela cell (ii), and breast cancer-MDAMB231 cell (iii)



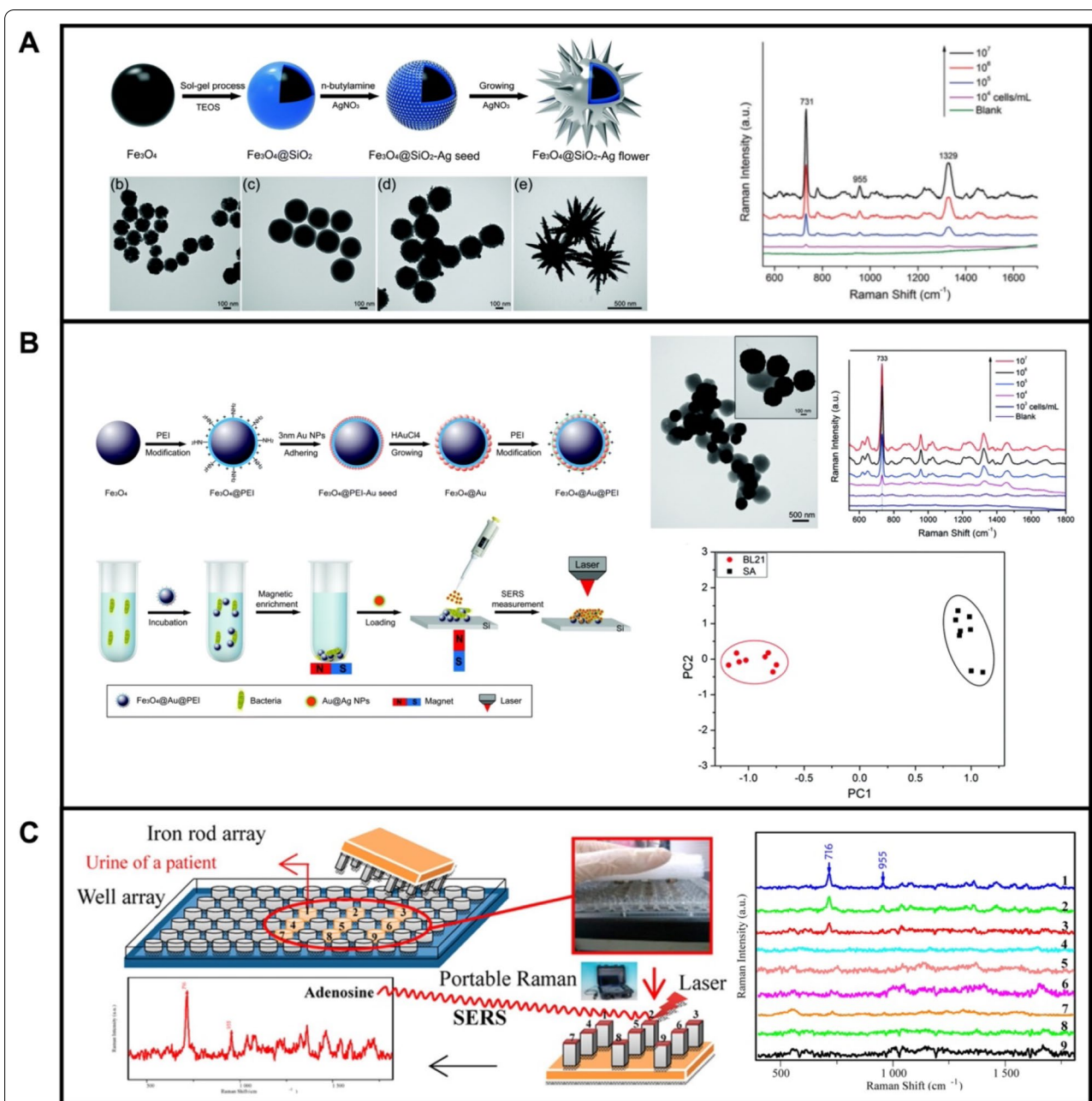
connected with the Q-structured  $\text{TiO}_x$  semiconductor and corresponding SERS spectra show the differences among the diverse types of cells.

The  $\pi$ -conjugated carbon structure of organic semiconductors imparts such materials with excellent biocompatibility to perform SERS sensing of biological samples [7, 190, 191]. Ganesh et al. [192] synthesized organic semiconductors as SERS substrates for investigating the epigenetic profile of cancer stem cells (Fig. 7C). The organic semiconductor is synthesized using an ultra-short, pulsed laser under a nitrogen gas environment, which enabled the shrinking of the organic semiconductor into a quantum scale. Such quantum scale endows the organic semiconductor with increased charge carrier mobility, which is necessary for efficient charge transfer in SERS. TEM observation revealed the particle size distribution of the organic semiconductor, with a diameter of 3.4 nm, which is in the quantum scale. Importantly, such organic semiconductors have high SERS activity with a  $10^{12}$

enhancement factor. Epigenetic analysis of fibroblast cells (NIH3T3), breast cells (MDA-MB231), pancreatic cancer (AsPc-1), and lung cancer (H69-AR) cells was conducted. As shown in Fig. 7C (right part), genomic DNA of different cell lines had different peak intensities due to the differences in base composition.

#### Indirect cancer and pathogens diagnosis based on SERS tags

The complexity of biological samples prevents direct SERS detection of a myriad of biomarkers, a cancer cell, or bacteria. To solve such a problem, indirect detection is performed using Raman tags that can interact specifically with the analyte, providing strong Raman signals. A representative SERS tag includes Raman enhancement nanomaterials, a Raman reporter, specific capture elements, and an internal standard [193, 194]. In some cases, SERS tags can experience random aggregation or degradation in complex samples at extreme pHs or ionic strength conditions. To avoid such a problem,

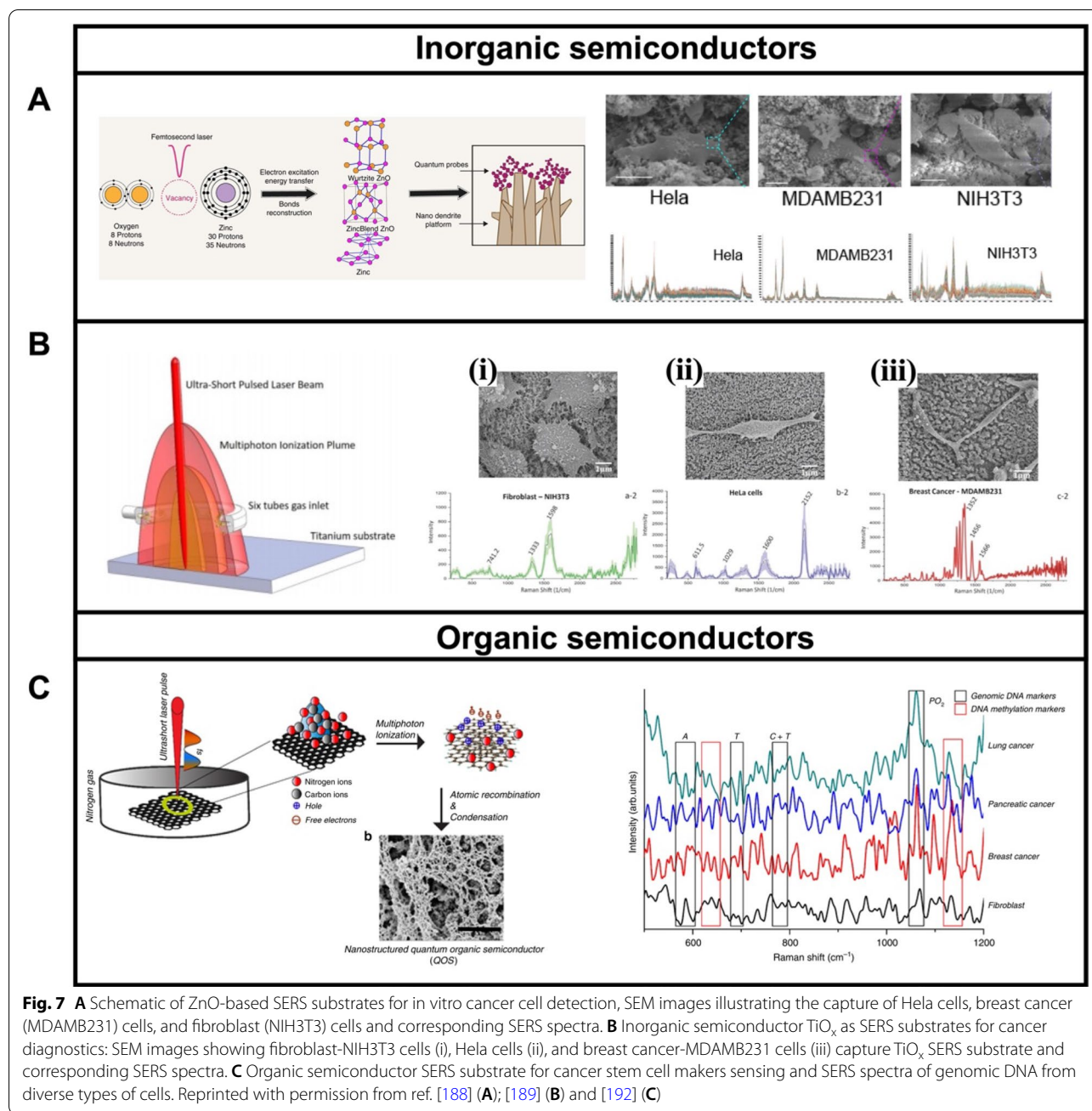


**Fig. 6** **A** Highly branched flower-like  $\text{Fe}_3\text{O}_4@SiO_2@Ag$  nano-hybrid for bacteria detection: Schematic of the synthesis of  $\text{Fe}_3\text{O}_4@SiO_2@Ag$  micro-flowers and corresponding SEM images at each step and SERS spectra for the detection of different concentrations of *Staphylococcus Aureus* using the nano-hybrid; **B** Schematic of the synthesis of PEI-modified nano-hybrids for the capture and enrichment of bacteria, SEM of  $\text{Fe}_3\text{O}_4@Au@PEI$ -*Escherichia coli* complex and corresponding SERS spectra and PCA differentiation between *Escherichia Coli* BL21 and *Staphylococcus Aureus* 24018. **C** Schematic illustration of  $\text{Fe}_3\text{O}_4/Au/Ag$  nano-hybrids for adenosine sensing and SERS spectra illustrating the detection with the sensing array (**B**) Reprinted with permission from ref. [171] (**A**); [95] (**B**) and [172] (**C**).

the particle can be coated with silica sols [195] or polystyrene shells [196], for enhanced stability. Dopamine or  $SiO_2$  shells also can enhance the biocompatibility of SERS tags, thus reducing cytotoxicity in disease diagnosis in clinical samples [197, 198].

### Raman reporter

Raman reporters are basic elements for designing efficient SERS tags and should possess the following characteristics: (A) stable and intense Raman signal; (B) clean spectral region with specific peaks; (C) ability to combine



**Fig. 7** **A** Schematic of ZnO-based SERS substrates for in vitro cancer cell detection, SEM images illustrating the capture of HeLa cells, breast cancer (MDAMB231) cells, and fibroblast (NIH3T3) cells and corresponding SERS spectra. **B** Inorganic semiconductor  $\text{TiO}_x$  as SERS substrates for cancer diagnostics: SEM images showing fibroblast-NIH3T3 cells (i), HeLa cells (ii), and breast cancer-MDAMB231 cells (iii) capture  $\text{TiO}_x$  SERS substrate and corresponding SERS spectra. **C** Organic semiconductor SERS substrate for cancer stem cell makers sensing and SERS spectra of genomic DNA from diverse types of cells. Reprinted with permission from ref. [188] (A); [189] (B) and [192] (C)

with Raman enhancement-related materials. Rhodamine (Rh6G) [199], crystal violet [196], malachite green [200], 5,5-dithiobis-2-nitrobenzoic acid (DTNB) [201], methylene blue (MB) [202], p-amino thiophenol (PATP) [203], etc., have been widely employed as Raman reporters for the fabrication of SERS tags.

#### Internal standard (IS)

An internal standard is a stable substance added in constant amounts to the samples and calibration solutions

for reliable and quantitative detection. By the employment of an internal standard, the variations from the uneven EM or CM enhancement, as well as other inaccuracies such as instrumental variations will be reduced. IS used for SERS sensing should have the following properties: (a) uniform dispersion on SERS substrate [204]; (b) the signal intensities should be comparable to the sensing targets, with one band in the silent regions of the sensing target [205]. Different organic molecules such as  $\beta$ -mercaptoethylamine, 4-mercaptobenzoic acid,

mercaptopyridine, etc., have been used as SERS internal standards [206]. Especially, Raman peaks from the SERS substrate can be used as IS. For example, Zou et al. [207] employed graphitic nanomaterials as IS due to their unique, strong, and stable Raman peaks localized in the silent Raman region of the sensing targets. Zhang et al. [208] fabricated carbon nanotube/Ag nanoparticle composites (CNT/AgNPs) as SERS substrates, with carbon nanotube acting as IS for the calibration of the intensity of the SERS targets. As a result, the integration of IS into the SERS substrate provides a reliable way for quantitative SERS detection of targets, which is important for the realization of clinical applications.

### SERS Tags

By incorporating a Raman reporter, the SERS tag can provide a Raman signal with high stability and intensity. Specific capture probes can be used for target delivery and interaction with the analyte of interest. The capture element can be categorized into the following groups [1, 27, 209]: (A) antibody, which is a Y-shaped protein that is widely used in recognizing antigens with high efficiency and specificity. However, they always suffer from low stability and high cost [210, 211]; (B) aptamer, which is DNA or RNA that can specifically bind to the target, acting as a cheap, stable, and highly specific recognition element. Yet, the limited selection for targets, cross-reactivity and stability issues (due to its small size) makes aptamers much less popular than antibodies, especially for clinical applications [212, 213]; (C) molecularly imprinted polymer (MIPs), which are prepared by using molecular imprinting technique, leaving cavities in the polymer with high specificity for the chosen “template” molecule. Such recognition elements are cheap and can be used in compartments at extreme (pH, temperature) conditions [214]; (D) antibiotic, which is used for the inactivating/killing of bacteria. Such capture elements also possess superiorities such as cheap, chemically stable, and high production rate, still, they are only special for the recognition of different types of bacteria, with limited selectivity for different bacterial strains [215]; (E) other recognition elements [216–218] such as transferrin are also used for the targets capture due to the overexpression of related receptors on cancer cell surfaces. Cancer and pathogens diagnosis strategies using several types of recognition elements and SERS detection are listed in Table 4.

Beqa et al. [219] prepared Au nano-popcorn/SWCNTs nanohybrids for theragnostic applications. Figure 8A shows the schematic of the fabrication process, in which SWCNTs were functionalized with sulfhydryl- groups, followed by Au nano popcorn attachment onto the nanotube surfaces via an Au–S bond. In the following step,


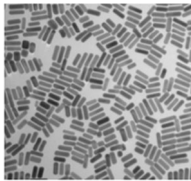
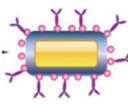
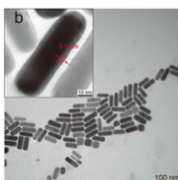
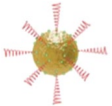
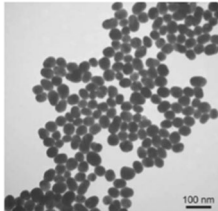
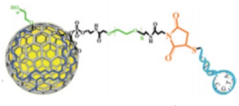
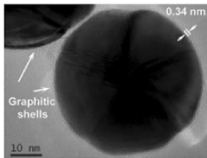
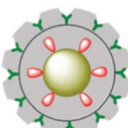
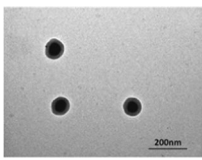
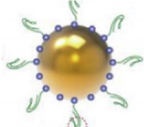
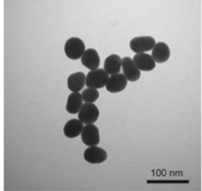

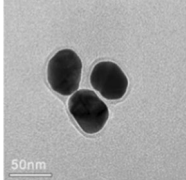
the S6 aptamer with sulfhydryl- group was attached to the nano-hybrid. This nano-hybrid show superior performance in the sensing of SK-BR-3 cancer cells. After Au nano-popcorn were adsorbed onto the SWCNTs surfaces, the Raman signal from SWCNTs (D band,  $1300\text{ cm}^{-1}$ ; G band,  $1590\text{ cm}^{-1}$ ) increased by an order of magnitude. Importantly, the SK-BR-3 cancer cell can induce the aggregation of the aptamer-modified nano-hybrid to generate hot spots. The strategy is highly specific as revealed in the low Raman signal enhancements in the presence of other cells (MDA-MB or HaCaT normal skin cells). Wang et al. [220] modified SWCNTs with Ag or AuNPs for cancer cell imaging. As depicted in Fig. 8B, the SWCNTs were modified with DNA, followed by seed growth of the NPs to generate the SWCNT-Ag or SWCNT-Au nano-hybrids. The surfaces of the as-prepared nano-hybrids were further modified with polyethylene glycol (PEG) to improve the stability in physiological conditions. Next, the authors modified the nano-hybrid with folic acid (FA) for specific attachment of human carcinoma KB cells and cell imaging. As expected, KB cells incubated with FA-modified nano-hybrid showed apparent Raman signals, while Hela cells show no obvious Raman signals.

### Clinical translation of SERS-based cancer and pathogens diagnosis: current advantages and challenges

#### Enhanced robustness and reproducibility of Raman signal enhancement

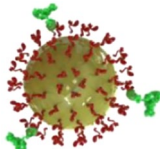
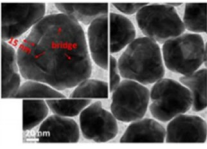
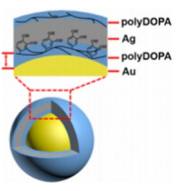
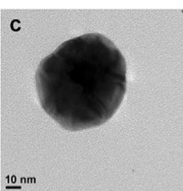
One important limitation of SERS detection that hampers the translation from laboratory to the clinical setting is their robustness and reproducibility. Significant efforts had been aimed to address this issue through the following methods: (1) The introduction of ordered SERS substrates. A SERS substrate with a highly regular structure is the key to producing uniform Raman signal enhancement, ensuring thus the accuracy and reproducibility in clinical applications. For instance, Kim et al. [221] sputtered a monolayer polystyrene nanosphere with a gold layer to form regularly arranged nanostructures. The periodic structure can function as a SERS substrate with <5% relative standard deviation for high reliability and reproducibility. Later, tear fluids from breast cancer patients and control groups were measured by a handheld Raman spectrometer with the as-fabricated periodic SERS substrate, with a clinical sensitivity of 92% and a specificity of 100% for breast cancer identification. Yet, it is unclear if the biomarkers are related to cancer, since further validation is missing. Zhu et al. [222] employed periodic arrays (hexagonal-packed gold film over nanosphere, AuFON) to improve the reproducibility of detection. In addition, the hydrophilic/hydrophobic

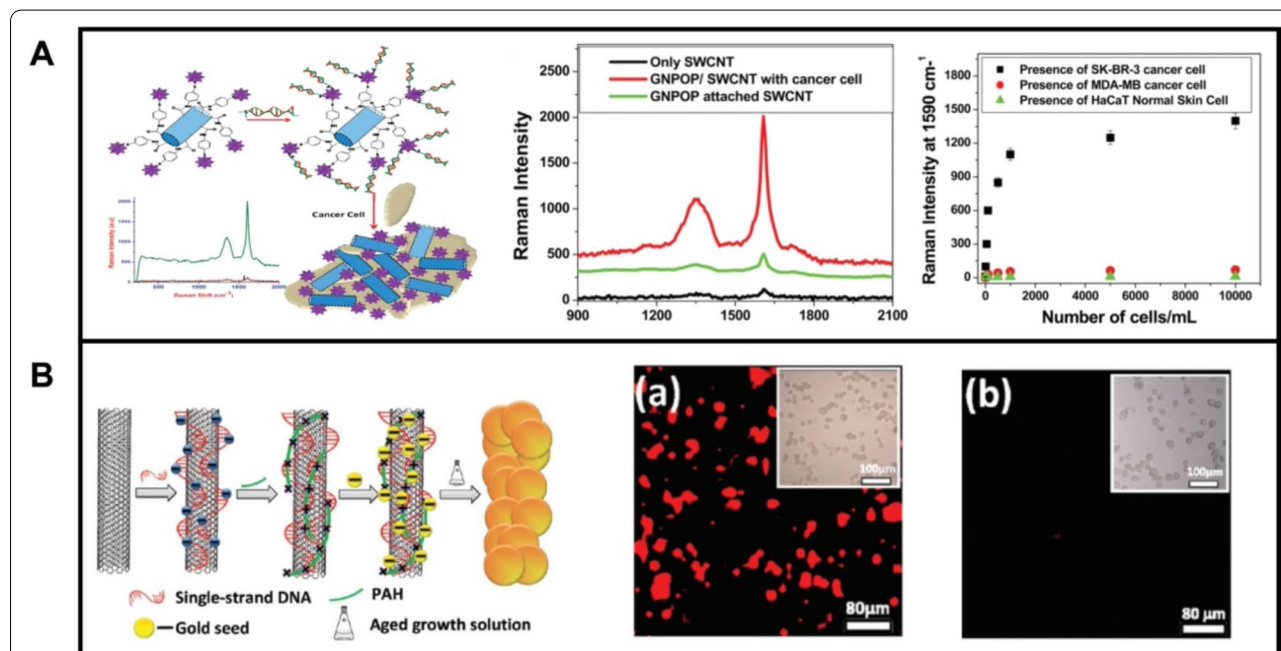
**Table 4** SERS tags using different specific recognition elements for indirect cancer and pathogens diagnosis

Recognition elements	SERS Tags		Reporter	Target analyte/cells	Refs.
	Structure	Morphology			
Antibody	 <p>Antibody-DTNB-Au nanorod</p>		DTNB	<i>Staphylococcus aureus</i>	[210]
	 <p>Antibody-DTNB-Au@Ag nanorod</p>		DTNB	Circulating tumor cells	[211]
Aptamer	 <p>Aptamer-conjugated Au</p>		DTNB, MBA	<i>Escherichia Coli</i> <i>Staphylococcus aureus</i>	[212]
	 <p>Aptamer-DSPE-graphene isolated Au nanocrystals (GLANs)</p>		2D carbon nanomaterials	HepG2, A549 cell lines	[213]
MIPs	 <p>MIP-PATP-Ag nanoparticles</p>		PATP	Sialic acid (cancer cells and tissues imaging)	[214]
Antibiotic	 <p>Vancomycin (Van)-MBA-Au</p>		MBA	<i>Staphylococcus aureus</i>	[215]
Luteinizing hormone-releasing hormone (LHRH)	 <p>LHRH-pMBA-Au nanoparticles</p>		4-mercaptobenzoic acid (pMBA)	Circulating tumor cells	[216]



**Table 4** (continued)

Recognition elements	SERS Tags		Reporter	Target analyte/cells	Refs.
	Structure	Morphology			
Transferrin			1,4-benzenedi-thiol (BDT)	Hela cell	[217]
Folic acid	 FA-Au@polyPOPA@Ag		Rh6G MB	Human lung adenocarcinoma cell line A549	[218]



**Fig. 8** **A** Au nano popcorn modified SWCNTs nano-hybrid for specific diagnosis of SK-BR-3 cancer cells. The left part shows the schematic illustration in the synthesis procedure their application in cancer cell diagnosis; middle part shows the Raman spectra of SWCNTs, Au nano popcorn modified SWCNTs nano-hybrid, and Au nano popcorn modified SWCNTs nanocomposites decorated with SK-BR-3 cancer cell and the right part the SERS intensity changes at  $1590\text{ cm}^{-1}$  after the addition of different amounts of SK-BR-3, MDA-MB human breast cancerous, and HaCaT normal skin cells to the aptamer modified nano-hybrid. **B** Schematic illustration of the synthesis of SWCNT-Ag-PEG-FA or SWCNT-Au-PEG-FA nano-hybrids for specific Raman imaging of KB cells and Raman images of SWCNT-Au-PEG-FA incubated with KB cells (middle part) and HeLa cell (right part). Reprinted with permission from ref. [219] (A) and [220] (B)

character of the SERS substrate endows the platform with reduced nonspecific adsorption, which is important for lateral accurate and sensitive detection. Direct detection in blood can be achieved. (2) The introduction of SERS tags. The encoding of Raman reporters into the

plasmonic metal to function as SERS tags could improve the stability, specificity, and uniformity of Raman signal enhancement. Bai et al. [223] designed SERS tags using AuNPs as SERS substrate and 3 different molecules with specific narrow Raman bands in the bio-silent region

as reporters. With further antibody modification, the immunoassay of 3 different liver cancer antigens including  $\alpha$ -fetoprotein (AFP), carcinoembryonic antigen (CEA), and ferritin (FER) was conducted in 39 clinical serum samples. (3) The introduction of IS. A reliable quantitative detection method also is necessary for clinical applications. To address this issue, the employment of an internal standard could effectively calibrate the variations from the uneven EM or CM enhancement, as well as other inaccuracies such as instrumental variations. Lin et al. [224] developed a label-free SERS-based method for DNA detection. SERS signals from the phosphate backbone were used as IS to improve the accuracy in the quantitative analysis of DNA. Such a method has been successfully employed for circulating DNA sensing, with good sensitivity and specificity for differentiating nasopharyngeal cancer patients from normal subjects.

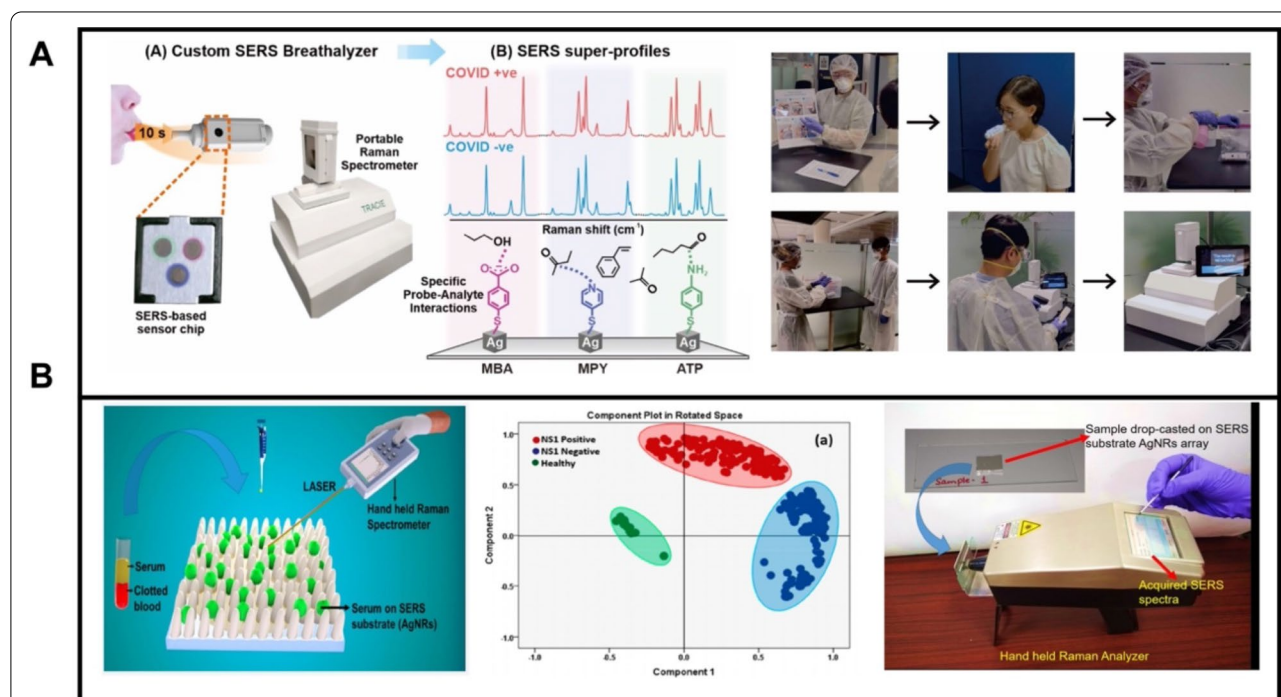
**Portable Raman spectrometers for clinical translation**

Traditional Raman measurements for SERS detection needs to be conducted in a special laboratory due to the enormous size of the equipment, which will restrict its real applications for clinical translation. As a solution for portable detection, Leong et al. [225] developed a hand-held SERS breathalyzer to identify Coronavirus disease 2019 (COVID-19) individuals through the detection of

volatile organic compounds (BVOCs) in breath (Fig. 9A). Multiple molecular receptors were employed to capture BVOCs in exhaled breath and acquire specific spectral variations between COVID-positive and COVID-negative individuals (middle part). The SERS-based breathalyzer allows for fast and noninvasive screening with high sensitivity and specificity for COVID-19 detection. Gahlaut et al. [32], developed a SERS-based diagnosis of dengue virus in blood samples. Silver nanorod array were used as SERS substrates (Fig. 9B). With the employment of a hand-held Raman spectrometer, such detection could be conducted in the field wherever needed, which is important in the clinical diagnosis (right part). They also demonstrate SERS diagnosis of dengue virus in blood samples collected from 102 subjects, successfully validating the approach.

**Machine learning methods for clinical translation**

In the direct detection of cancer or pathogens, specific fingerprints from the vibration of molecules may suffer from subtle differences which are difficult to be identified by manual visual inspection. Therefore, machine learning which is part of artificial intelligence (AI), has been integrated into SERS detection to identify features or perform classification. Due to the power of machine learning methods, information could be extracted effectively



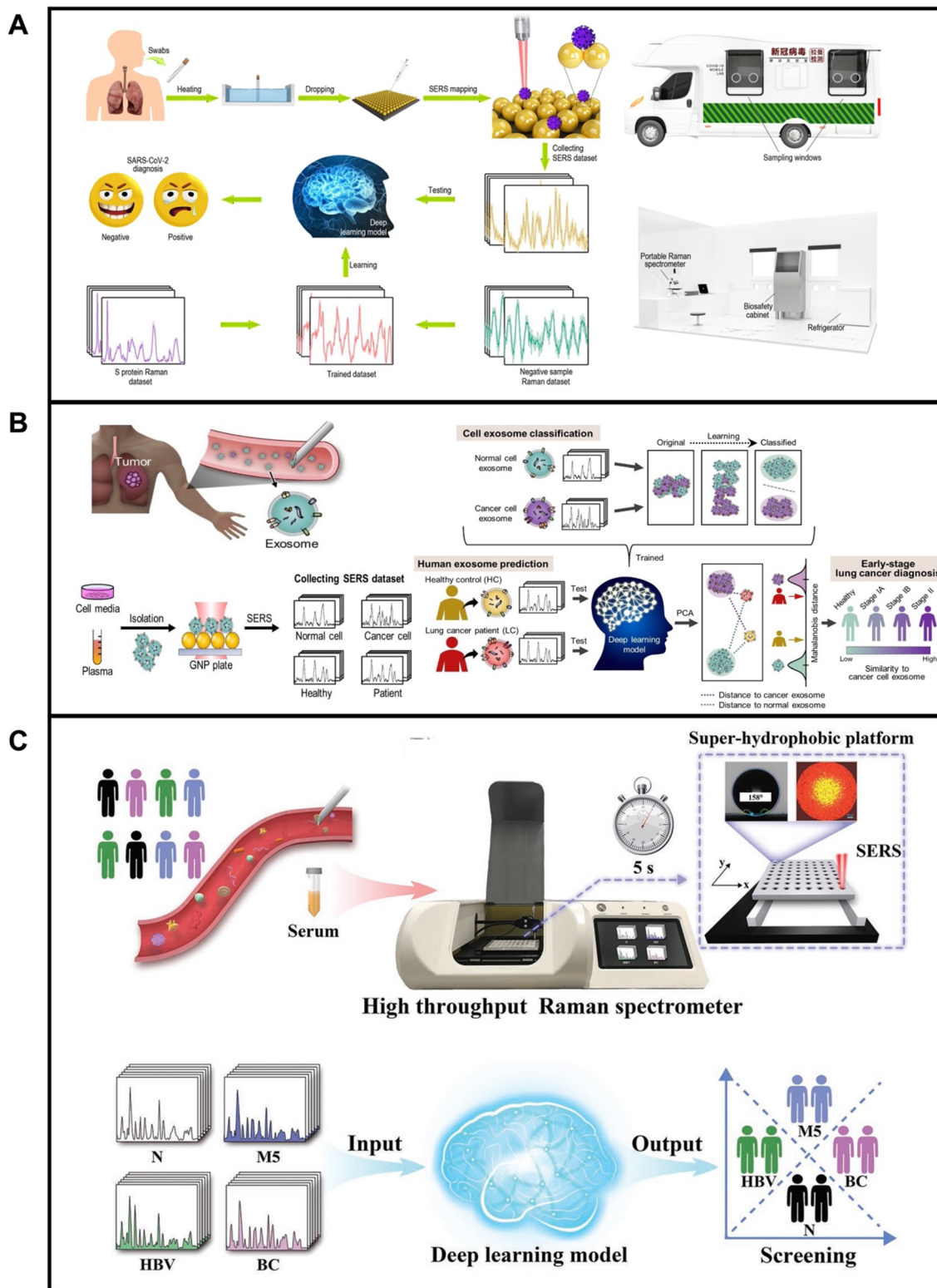
**Fig. 9** **A** SERS-based breathalyzer for mass screening of COVID-19, schematic of the interaction of different molecular receptors interacts with BVOCs, and photographs describing the participant recruitment workflow. **B** Silver nanorod array for dengue diagnosis in blood samples using a hand-held Raman spectrometer and PCA discrimination. Reprinted with permission from ref. [225] (A) and [32] (B)

from the vibrational spectra of complex mixtures or big datasets, which promotes the translation of SERS from proof-of-concept to clinical applications [226]. The most usual form of machine learning is the supervised learning methods, which include a discriminant analysis-based method, artificial neural network, k-nearest neighbor, etc. This model learns by extracting knowledge from the raw data and using this as-obtained knowledge to make decisions from unknown samples [227]. Unsupervised learning algorithms have been also introduced and compared with their supervised counterparts [228]. Huang et al. [229] employed AuNPs array as SERS substrates for label-free detection of SARS-Cov-2. Due to the nail-like shape of the virus, the spike (S) protein has the maximum probability to interact with the hot SERS spots and was thus chosen as the detection target. In the lateral clinical applications, a deep-learning algorithm of pure S protein and negative clinical specimens was used in the rapid screening of SARS-CoV-2 antigen, with an identification accuracy of 87.7% (Fig. 10A). In addition, a portable Raman spectrometer was used to conduct the detection, pre-treatment, and spectra measurements. While promising, the overall accuracy of the detection should be improved. Shin et al. [230] used a deep learning-based computer algorithm to overcome the complexity and heterogeneity in analyzing the SERS signal of exosomes in blood (Fig. 10B). After collecting the Raman signals of exosomes using an AuNPs-coated plate as a SERS substrate, the as-obtained spectral dataset is used to train the deep learning models (right part). In a prediction of 43 cancer patients, they also show good results by the integration of SERS analysis and deep learning model, which means a promising method for the early-stage liquid biopsy of lung cancer. Still, the method is limited by the lack of validation studies or additional biomarker identification. Because circulating biomarkers from tumors in these biofluids are very scarce and most biomolecules are from non-tumor origins, careful considerations should be made to ensure the separation is not due to overfitting. Lin et al. [231] employed super-hydrophobic substrates in connection with deep learning techniques for developing high throughput, a label-free analytical platform for disease screening (Fig. 10C). In this work, an aluminum plate with a super-hydrophobic groove was specially designed to prevent the coffee ring effect and promote the self-localization of the droplet. The SERS platform was then applied for serum sample detection containing breast cancer (BC), hepatitis B virus (HBV), and leukemia M5 (M5) patients. The deep learning model was trained to statistical analysis the SERS spectral data from clinical samples to classify large and complicated fingerprints of target molecules, which is important for efficient large-scale population cancer screening.

During the past years we have witnessed the significant effort to translate SERS approaches from the laboratory to clinical use, which is a promising option for future cancer and pathogen detection. Yet, critical issues still need to be considered: (1) Direct measurements have the advantage of showing some chemical information, yet related works fail to provide what biomarkers were detected, which are important to explain why these changes in Raman peaks are related to diseases, as well as the further validation of the findings. Therefore, further studies related to direct detection should go deep into the identification of related biomarkers and include interdisciplinary validation studies. (2) In promoting clinical translation, even though SERS substrates are designed into periodic structures to improve the uniformity for Raman signal enhancement, massive cancer, or pathogen disease screening is restricted to the small cohort sizes of the SERS substrate. Hence, scientists should focus more on the fabrication of large-scale periodic SERS substrates. (3) Recent progress proved that SERS could be utilized in large-scale COVID-19 screening, with fast, high sensitivity and specificity. Yet, sample collection by breathalyzer may face drawbacks. Compare with traditional throat swabs where sample collection is conducted by the doctor, participants will need to conduct the breathalyzer themselves where the doctors must explain what they need to do. It is also hard to ensure the amounts of exhalations to keep similar among different people. In addition, so many people blowing at the same place may increase the risk of cross-infectious.

### Conclusion and prospect

Cancer and pathogens are now the major causes of death around the world, thus the development of simple, rapid, and effective diagnostic tools. Driven by the development of optical and material science, SERS have shown immense potential for disease diagnosis, including cancer cells, microorganism, and related biomarkers sensing. In this review, we have discussed recent advances in SERS-based strategies for cancer and pathogens diagnosis via direct and indirect ways. In the direct detection mode, despite SERS-based strategies have provided quick, sensitive, and basic chemical structures of target molecules for disease diagnosis, Raman signal enhancement is an overly complex phenomenon and depend on the nanomaterials size, aggregation degree, and analyte/substrate interaction mode. Therefore, the clinical application needs to focus on the reproducibility of signal output in the quantification of disease targets. As signal amplification of analyte depends on the strength of the EM field that is distributed around plasmonic nanomaterials with remarkable differences, even the same molecule close to different positions of the nanomaterials



**Fig. 10** **A** Detection of SARS-CoV-2 antigens by deep learning-based SERS technology. The left part is a schematic illustration of the working flow; the right part is a schematic illustration of the SERS mobile detection platform. **B** Deep learning-based circulating exosome analysis for lung cancer diagnosis, left part show circulation of lung cancer tumor exosomes in the bloodstream and schematic illustration of the collection of SERS spectroscopy of exosomes; right part reveals that spectral dataset is used to train the deep learning models. Reprinted with permission from ref. [229] (A) and [230] (B) and [231] (C)

will lead to different signal intensity output. In addition, EM field distribution from different signal nanoparticles interacts with each other when two nanoparticles are getting close to a specific distance. Hence, the EM field distribution of whole aggravated nanoparticles is different from that arising from a single nanoparticle [232–234]. The use of IS is another strategy to simplify quantitative SERS analysis, in which unstable signals from the inhomogeneous distribution of the EM field will be corrected by the internal peaks [207, 235, 236]. Direct SERS detection also provides chemical information of the targets, which could function as a “*finger-print*” for direct bacteria or cancer cell identification. Yet in cases, the subtle differences from their specific Raman spectra are hard to identify. To solve this problem, machine learning has been used to identify features or perform classification, in which information could be extracted effectively from the complex mixtures or big datasets, thus helping in disease diagnosis or screening in clinical applications [229, 230, 237, 238]. In the indirect detection mode, Raman reporters, enhancement nanomaterials, vibrational spectra, and specific recognition elements are integrated into one SERS tag, which can capture targets and provide strong and identical Raman signals with high sensitivity and specificity. Though the indirect detection mode will lose the natural information of chemicals, the employment of SERS tags enables the promising detection of targets from complex real samples, which is important for clinical applications [223, 239].

Another important challenge that still requires attention is the biocompatibility of SERS substrates for living cancer and pathogens cells imaging, or in-vitro analyte monitoring. The most used plasmonic metal (Ag, Au, Cu, etc.) possess high cytotoxicity and thus may cause changes in cell structures (target protein or other organic chemicals) and influence the mapping/sensing results. The coating of metal nanomaterials with biocompatible materials such as polyethylene glycols [240], SiO<sub>2</sub> [198], etc. can reduce their cytotoxicity. However, the coating of the biocompatible membrane may hamper the Raman enhancement ability of the SERS substrate [241]. Integration of carbon materials such as graphene also can reduce the cytotoxicity of metals [242], still, the total size of nano-hybrid needs to be considered due to the optimal nanomaterial radius for endocytosis is about 25–30 nm [243]. Therefore, further efforts still should have focused on the fabrication of SERS substrates with good biocompatibility and SERS activity.

The development of portable and miniature SERS platforms is also important to expand the applicability of disease diagnosis with higher realistic scenarios. Current attempts such as portable Raman devices [244] and microfluidic platforms [245], etc., make disease diagnosis

more flexible, still, traditional SERS techniques are widely used in cancer and pathogens diagnosis due to their superior SERS performance such as sensitivity, spectral resolution, and mapping functionality. As detail described above, portable devices already have been successfully utilized in the screening of COVID-19 individuals in clinical breath samples or dengue virus in clinical blood samples. Such works have fully proven the effectiveness of portable devices in the realization of clinical translation, as well as enormous potential in the development of noninvasive human diagnostic tools for point-of-care detection or mass screening purposes. Therefore, further efforts still need to focus on realizing disease diagnosis in a portable way to meet clinical needs.

Lastly, the combination of SERS and other technologies also shows great potential in promoting SERS detection from proof-of-concept to clinical translation, which includes: (1) The coupling between electrochemistry (EC) and SERS, in which chemical enhancement could be strengthened by EC, as well as molecules may be captured (while molecular charge and electrode potential are at appropriate state) by substrate/electrode to get closer to the strong electromagnetic field, hence results in higher Raman signal enhancement. Importantly, the integration of EC makes molecular adsorption on substrate/electrode with high uniformity and brief time, which is important for further quantitative analysis and clinical applications [246]. (2) The integration of SERS onto a flexible substrate to function as wearable sensors. Wearable sensors have made great progress in recent years. Due to their advantages such as the capability of remote monitoring and continuous detection, as well as high biocompatibility and wearability, wearable devices also show great promise in advancing SERS into clinical applications [247, 248]. (3) The employment of micro/nanomotor for enhanced sensitive and rapid SERS detection. Current SERS substrates mostly can only interact with targets through free diffusion of the molecules or nanoparticles themselves which would limit the effective recognition between the analyte and related active surfaces, thus resulting in confined detection speed and sensitivity. The micro/nanomotor are fabricated micro/nano actuators that could transform outside energies into their mechanical motion. Diverse types of energy such as chemical energy, light, ultrasound, or magnetic energy could be used in micro/nanomotor propulsion. By the integration of micro/nanomotor, the above-mentioned problems in SERS detection would be well solved and help in the realization of clinical translation [249, 250].

#### Abbreviations

SERS: Surface enhanced Raman scattering; EM: Electromagnetic enhancement; CM: Chemical enhancement; EF: Enhancement factor; MoS<sub>2</sub>:

Molybdenum disulfide; 3D: Three dimension; SEM: Scanning-electron microscopy; LOD: Limit of detection; EV71: Enterovirus 71; TEM: Transmission electron microscopes; DENV: Dengue virus; AuNRs: Gold nanorods; PEG: Polyethylene glycol; RGD: Arg-Gly-Asp; NLS: Nuclear localization signal; NIR: Near infrared spectroscopy; CFU: Colony-forming unit; PEI: Polyetherimide; RNA: Ribonucleic acid; DNA: Deoxyribonucleic acid; NPs: Nanoparticles; *E. coli*: *Escherichia coli*; BN: Boron nitride; BP: Black phosphorous; G@AgNPs@Si: Graphene-silver nanoparticles-silicon; Ag@NGO: Graphene oxide coated with silver nanoparticles; WS<sub>2</sub>: Tungsten disulfide; g-C<sub>3</sub>N<sub>4</sub>: Graphitic carbon nitride; CNTs: Carbon nanotubes; SWCNTs: Single-wall carbon nanotubes; MWCNTs: Multi-wall carbon nanotubes; FA: Folic acid; C-dot-Ag-NP: Carbon-dot/silver-nanoparticle; PDMS: Polydimethylsiloxane; C-dots: Carbon dots; HAUCl<sub>4</sub>: Chloroauric acid; ATP: Adenosine triphosphate; NSL: Nanosphere lithography; EBL: Electron beam lithography; CTCs: Circulating tumor cells; RSV: Respiratory viruses; PCV2: Porcine circovirus 2; PRV: Pseudorabies virus; H5N1: Influenza A; Fe<sub>3</sub>O<sub>4</sub>: Iron Oxide; CuO: Copper(II) oxide; MnFe<sub>2</sub>O<sub>4</sub>: Manganese Iron Oxide; ZnO: Zinc oxide; CoFe<sub>2</sub>O<sub>4</sub>: Ni: Nickel; FePt: Iron-platinum; CoPt: Cobalt-platinum; SiO<sub>2</sub>: Silicon dioxide; PCA: Principal component analysis; Rh6G: Rhodamine 6G; DTNB: 5,5-Dithiobis-2-nitrobenzoic acid; MB: Methylene blue; PATP: P-aminothiophenol; MIPs: Molecularly imprinted polymer; pMBA: 4-Mercapto-benzoic acid; BDT: 1,4-Benzenedi-thiol; LHRH: Luteinizing hormone releasing hormone; GLANs: Aptamer-DSPF-graphene isolated Au nanocrystals.

#### Acknowledgements

Not applicable.

#### Author contributions

KY, BJS, and AE conceptualization, writing, and original draft preparation, review, and editing; BJS and AE supervision; funding acquisition. All authors read and approved the final manuscript.

#### Funding

This research was funded by the Spanish Ministry of Economy, Industry and Competitiveness [Grant Numbers RYC-2015-17558, co-financed by EU (B.J.S)], Grant PID2020-118154GB-I00 funded by MCIN/AEI/10.13039/501100011033 (A. E and B.J.S.); the Community of Madrid [Grant Numbers CM/JIN/2021-012 (B.J.S), TRANSNANOAVANSENS, S2018/NMT-4349 (A.E)]. B. J.S. and A. Escarpa acknowledge funding from DISCOVER-UAH-CM Project (Ref. REACT UE-CM2021-01), co-founded by Community of Madrid (CAM) and European Union (UE), through the European Regional Development Fund (ERDF) and supported as part of the EU's response to COVID-19 pandemic. K. Yuan acknowledge funding from SUMC Scientific Research Initiation Grant (Grant Number 510858045).

#### Availability of data and materials

Not applicable.

#### Declarations

#### Ethics approval and consent to participate

Not applicable.

#### Consent for publication

Not applicable.

#### Competing interests

The authors declare that they have no competing interests.

#### Author details

<sup>1</sup>Bio-Analytical Laboratory, Shantou University Medical College, No. 22, Xinling Road, Shantou 515041, China. <sup>2</sup>Department of Analytical Chemistry, Physical Chemistry, and Chemical Engineering, University of Alcalá, Alcalá de Henares, 28802 Madrid, Spain. <sup>3</sup>Chemical Research Institute "Andrés M. del Río", University of Alcalá, Alcalá de Henares, 28802 Madrid, Spain.

Received: 27 May 2022 Accepted: 15 November 2022

Published online: 22 December 2022

#### References

- Yuan K, Jiang Z, Jurado-Sánchez B, Escarpa A. Nano/micromotors for diagnosis and therapy of cancer and infectious diseases. *Chem Eur J*. 2020;26:2309–26.
- Schiffman JD, Fisher PG, Gibbs P. Early Detection of cancer: past, present, and future. *Am Soc Clin Oncol Educ Book*. 2015;35:57–65.
- Delgado-Viscogliosi P, Solignac L, Delattre J-M. Viability PCR, a culture-independent method for rapid and selective quantification of viable *Legionella pneumoniae* cells in environmental water samples. *Appl Environ Microb*. 2009;75:3502.
- Davenport M, Mach KE, Shortliffe LMD, Banaei N, Wang TH, Liao JC. New and developing diagnostic technologies for urinary tract infections. *Nat Rev Urol*. 2017;14:296–310.
- Cialla-May D, Zheng XS, Weber K, Popp J. Recent progress in surface-enhanced Raman spectroscopy for biological and biomedical applications: from cells to clinics. *Chem Soc Rev*. 2017;46:3945–61.
- Li X, Ye S, Luo X. Sensitive SERS detection of miRNA via enzyme-free DNA machine signal amplification. *Chem Commun*. 2016;52:10269–72.
- Demirel G, Usta H, Yilmaz M, Celik M, Alidagi HA, Buyukserin F. Surface-enhanced Raman spectroscopy (SERS): an adventure from plasmonic metals to organic semiconductors as SERS platforms. *J Mater Chem C*. 2018;6:5314–35.
- Kneipp K, Ozaki Y, Tian ZQ. Recent developments in plasmon-supported Raman spectroscopy. *World Scientific (Europe)*. London; 2017.
- Fateixa S, Nogueira HIS, Trindade T. Hybrid nanostructures for SERS: materials development and chemical detection. *Phys Chem Phys*. 2015;17:21046–71.
- Guo H, He L, Xing B. Applications of surface-enhanced Raman spectroscopy in the analysis of nanoparticles in the environment. *Environ Sci Nano*. 2017;4:2093–107.
- Ren X, Cheshari EC, Qi J, Li X. Silver microspheres coated with a molecularly imprinted polymer as a SERS substrate for sensitive detection of bisphenol A. *Microchim Acta*. 2018;185:242.
- Bi L, Wang Y, Yang Y, Li Y, Mo S, Zheng Q, et al. Highly sensitive and reproducible SERS sensor for biological pH detection based on a uniform gold nanorod array platform. *ACS Appl Mater Interfaces*. 2018;10:15381–7.
- Joseph MM, Narayanan N, Nair JB, Karunakaran V, Ramya AN, Sujai PT, et al. Exploring the margins of SERS in practical domain: An emerging diagnostic modality for modern biomedical applications. *Biomaterials*. 2018;181:140–81.
- Hong Y, Zhou X, Xu B, Huang Y, He W, Wang S, et al. Optoplasmonic hybrid Materials for trace detection of methamphetamine in biological fluids through SERS. *ACS Appl Mater Interfaces*. 2020;12:24192–200.
- Shen J, Zhou Y, Huang J, Zhu Y, Zhu J, Yang X, et al. In-situ SERS monitoring of reaction catalyzed by multifunctional Fe<sub>3</sub>O<sub>4</sub>@TiO<sub>2</sub>@Ag-Au microspheres. *Appl Catal B: Environ*. 2017;205:11–8.
- Wang X, Du Y, Zhang H, Xu Y, Pan Y, Wu T, et al. Fast enrichment and ultrasensitive in-situ detection of pesticide residues on oranges with surface-enhanced Raman spectroscopy based on Au nanoparticles decorated glycidyl methacrylate–ethylene dimethacrylate material. *Food Control*. 2014;46:108–14.
- Smith WE. Practical understanding and use of surface-enhanced Raman scattering/surface-enhanced resonance Raman scattering in chemical and biological analysis. *Chem Soc Rev*. 2008;37:955–64.
- Moore TAO, Moody AS, Payne TD, Sarabia GM, Daniel AR, Sharma BAO. In vitro and in vivo SERS biosensing for disease diagnosis. *Biosensors*. 2018;8:2079–6374.
- Sinha SS, Jones S, Pramanik A, Ray PC. Nanoarchitecture-based SERS for biomolecular fingerprinting and label-free disease markers diagnosis. *Acc Chem Res*. 2016;49:2725–35.
- Maiti KK, Dinish US, Fu CY, Lee JJ, Soh KS, Yun SW, et al. Development of biocompatible SERS nanotag with increased stability by chemisorption of reporter molecule for in vivo cancer detection. *Biosens Bioelectron*. 2010;26:398–403.
- Vendrell M, Maiti KK, Dhaliwal K, Chang Y-T. Surface-enhanced Raman scattering in cancer detection and imaging. *Trends Biotechnol*. 2013;31:249–57.
- Wu X, Luo L, Yang S, Ma X, Li Y, Dong C, et al. Improved SERS nanoparticles for direct detection of circulating tumor cells in the blood. *ACS Appl Mater Interfaces*. 2015;7:9965–71.

23. Ding S-Y, You E-M, Tian Z-Q, Moskovits M. Electromagnetic theories of surface-enhanced Raman spectroscopy. *Chem Soc Rev*. 2017;46:4042–76.
24. Liu B, Thielert B, Reutter A, Stosch R, Lemmens P. Quantifying the contribution of chemical enhancement to SERS: A model based on the analysis of light-induced degradation processes. *J Phys Chem C*. 2019;123:19119–24.
25. Fan W, Yue-E M, Ling X, Liu T. Free-standing silver nanocube/graphene oxide hybrid paper for surface-enhanced Raman scattering. *Chin J Chem*. 2016;34:73–81.
26. Li X, Li J, Zhou X, Ma Y, Zheng Z, Duan X, et al. Silver nanoparticles protected by monolayer graphene as a stabilized substrate for surface-enhanced Raman spectroscopy. *Carbon*. 2014;66:713–9.
27. Chen J, Andler SM, Goddard JM, Nugen SR, Rotello VM. Integrating recognition elements with nanomaterials for bacteria sensing. *Chem Soc Rev*. 2017;46:1272–83.
28. Qiu Y, Deng D, Deng Q, Wu P, Zhang H, Cai C. Synthesis of magnetic Fe<sub>3</sub>O<sub>4</sub>-Au hybrids for sensitive SERS detection of cancer cells at low abundance. *J Mater Chem B*. 2015;3:4487–95.
29. Auner GW, Koya SK, Huang C, Broadbent B, Trexler M, Auner Z, et al. Applications of Raman spectroscopy in cancer diagnosis. *Cancer Metast Rev*. 2018;37:691–717.
30. Geen KG, Kumar D, Subrahmanyam S, Shanmugam K. Raman fingerprints in detection of breast cancer. *J Biosens Biomark Diagn*. 2016;1:1–11.
31. Han XX, Ozaki Y, Zhao B. Label-free detection in biological applications of surface-enhanced Raman scattering. *Trends Anal Chem*. 2012;38:67–78.
32. Gahlaut SK, Savargaonkar D, Sharan C, Yadav S, Mishra P, Singh JP. SERS platform for dengue diagnosis from clinical samples employing a handheld Raman spectrometer. *Anal Chem*. 2020;92:2527–34.
33. Wu L, Wang Z, Zhang Y, Fei J, Chen H, Zong S, et al. In situ probing of cell-cell communications with surface-enhanced Raman scattering (SERS) nanoprobes and microfluidic networks for screening of immunotherapeutic drugs. *Nano Res*. 2017;10:584–94.
34. Bodelón G, Montes-García V, López-Puente V, Hill EH, Hamon C, Sanz-Ortiz MN, et al. Detection and imaging of quorum sensing in *Pseudomonas aeruginosa* biofilm communities by surface-enhanced resonance Raman scattering. *Nat Mater*. 2016;15:1203–11.
35. Cao X, Wang Z, Bi L, Zheng J. Label-free detection of human serum using surface-enhanced Raman spectroscopy based on highly branched gold nanoparticle substrates for discrimination of non-small cell lung cancer. *J Chem*. 2018;2018:9012645.
36. González-Solís J, Luévano Colmenero G, Vargas-Mancilla J. Surface enhanced Raman spectroscopy in breast cancer cells. *Laser Ther*. 2013;22:37–42.
37. Cui S, Zhang S, Yue S. Raman spectroscopy and imaging for cancer diagnosis. *J Healthc Eng*. 2018;2018:8619342.
38. Nguyen BH, Nguyen VH, Tran HN. Rich variety of substrates for surface-enhanced Raman spectroscopy. *Adv Nat Sci Nanosci*. 2016;7: 033001.
39. Li X, Zhang J, Xu W, Jia H, Wang X, Yang B, et al. Mercaptoacetic acid-capped silver nanoparticles colloid: Formation, morphology, and SERS activity. *Langmuir*. 2003;19:4285–90.
40. dos Santos JDS, Alvarez-Puebla RA, Oliveira JON, Arca RF. Controlling the size and shape of gold nanoparticles in fulvic acid colloidal solutions and their optical characterization using SERS. *J Mater Chem*. 2005;15:3045–9.
41. Tian F, Conde J, Bao C, Chen Y, Curtin J, Cui D. Gold nanostars for efficient in vitro and in vivo real-time SERS detection and drug delivery via plasmonic-tunable Raman/FTIR imaging. *Biomaterials*. 2016;106:87–97.
42. Song C, Yang B, Zhu Y, Yang Y, Wang L. Ultrasensitive silver nanorod array SERS sensor for mercury ions. *Biosens Bioelectron*. 2017;87:59–65.
43. Kim DJ, Jeon TY, Park S-G, Han HJ, Im SH, Kim D-H, et al. Uniform microgels containing agglomerates of silver nanocubes for molecular size-selectivity and high SERS activity. *Small*. 2017;13:1604048.
44. Yan T, Zhang L, Jiang T, Bai Z, Yu X, Dai P, et al. Controllable SERS performance for the flexible paper-like films of reduced graphene oxide. *Appl Surf Sci*. 2017;419:373–81.
45. Shen Y, Miao P, Hu C, Wu J, Gao M, Xu P. SERS-based plasmon-driven reaction and molecule detection on a single Ag@MoS<sub>2</sub> microsphere: Effect of thickness and crystallinity of MoS<sub>2</sub>. *ChemCatChem*. 2018;10:3520–5.
46. Jiang R, Li B, Fang C, Wang J. Metal/semiconductor hybrid nanostructures for plasmon-enhanced applications. *Adv Mater*. 2014;26:5274–309.
47. He L, Liu C, Hu J, Gu W, Zhang Y, Dong L, et al. Hydrophobic ligand-mediated hierarchical Cu nanoparticles on reduced graphene oxides for SERS platform. *CrystEngComm*. 2016;18:7764–71.
48. Liang X, Liang B, Pan Z, Lang X, Zhang Y, Wang G, et al. Tuning plasmonic and chemical enhancement for SERS detection on graphene-based Au hybrids. *Nanoscale*. 2015;7:20188–96.
49. Wei H, Leng W, Song J, Willner MR, Marr LC, Zhou W, et al. Improved quantitative SERS enabled by surface plasmon enhanced elastic light scattering. *Anal Chem*. 2018;90:3227–37.
50. Fu HY, Lang XY, Hou C, Wen Z, Zhu YF, Zhao M, et al. Nanoporous Au/SnO/Ag heterogeneous films for ultrahigh and uniform surface-enhanced Raman scattering. *J Mater Chem C*. 2014;2:7216–22.
51. Wu LA, Li WE, Lin DZ, Chen YF. Three-dimensional SERS substrates formed with plasmonic core-satellite nanostructures. *Sci Rep*. 2017;7:13066.
52. Shi R, Liu X, Ying Y. Facing challenges in real-life application of surface-enhanced Raman scattering: Design and nanofabrication of surface-enhanced Raman scattering substrates for rapid field test of food contaminants. *J Agr Food Chem*. 2018;66:6525–43.
53. Lee HK, Lee YH, Koh CSL, Phan-Quang GC, Han X, Lay CL, et al. Designing surface-enhanced Raman scattering (SERS) platforms beyond hotspot engineering: emerging opportunities in analyte manipulations and hybrid materials. *Chem Soc Rev*. 2019;48:731–56.
54. Wu L, Wang W, Zhang W, Su H, Liu Q, Gu J, et al. Highly sensitive, reproducible and uniform SERS substrates with a high density of three-dimensionally distributed hotspots: gyroid-structured Au periodic metallic materials. *NPG Asia Mater*. 2018;10:e462–562.
55. Feng L, Li S, Li Y, Li H, Zhang L, Zhai J, et al. Super-hydrophobic surfaces: From natural to artificial. *Adv Mater*. 2002;14:1857–60.
56. Bhushan B. Adhesion of multi-level hierarchical attachment systems in gecko feet. *J Adhes Sci Technol*. 2007;21:1213–58.
57. Biró LP, Kertész K, Vértesy Z, Márk GI, Bálint Z, Lousse V, et al. Living photonic crystals: Butterfly scales - nanostructure and optical properties. *Mat Sci Eng C-Mater*. 2007;27:941–6.
58. Garrett NL, Sekine R, Dixon MWA, Tilley L, Bamberg KR, Wood BR. Bio-sensing with butterfly wings: naturally occurring nano-structures for SERS-based malaria parasite detection. *Phys Chem Chem Phys*. 2015;17:21164–8.
59. Zhang M, Meng J, Wang D, Tang Q, Chen T, Rong S, et al. Biomimetic synthesis of hierarchical 3D Ag butterfly wing scale arrays/graphene composites as ultrasensitive SERS substrates for efficient trace chemical detection. *J Mater Chem C*. 2018;6:1933–43.
60. Fabric L. SERS Tags: The next promising tool for personalized cancer detection? *ChemNanoMat*. 2016;2:249–58.
61. Guo M, Dong J, Xie W, Tao L, Lu W, Wang Y, et al. SERS tags-based novel monodispersed hollow gold nanospheres for highly sensitive immunoassay of CEA. *J Mater Sci*. 2015;50:3329–36.
62. Chen M, Zhang L, Gao M, Zhang X. High-sensitive bioorthogonal SERS tag for live cancer cell imaging by self-assembling core-satellites structure gold-silver nanocomposite. *Talanta*. 2017;172:176–81.
63. Pérez-Jiménez AI, Lyu D, Lu Z, Liu G, Ren B. Surface-enhanced Raman spectroscopy: benefits, trade-offs and future developments. *Chem Sci*. 2020;11:4563–77.
64. Scatena E, Baiguera S, Del Gaudio C. Raman spectroscopy and aptamers for a label-free approach: Diagnostic and application tools. *J Healthc Eng*. 2019;2019:2815789.
65. Pahlow S, Meisel S, Cialla-May D, Weber K, Rösch P, Popp J. Isolation and identification of bacteria by means of Raman spectroscopy. *Adv Drug Deliver Rev*. 2015;89:105–20.
66. Rinken T, Kivirand K. Biosensing technologies for the detection of pathogens: A prospective way for rapid analysis. *IntechOpen: Croatia*; 2018.
67. Zhang J, Ma X, Wang Z. Real-time and in-situ monitoring of Abrin induced cell apoptosis by using SERS spectroscopy. *Talanta*. 2019;195:8–16.

68. Zheng X-S, Jahn IJ, Weber K, Cialla-May D, Popp J. Label-free SERS in biological and biomedical applications: Recent progress, current challenges, and opportunities. *Spectrochim Acta A*. 2018;197:56–77.
69. Guo J, Liu Y, Chen Y, Li J, Ju H. A multifunctional SERS sticky note for real-time quorum sensing tracing and inactivation of bacterial biofilms. *Chem Sci*. 2018;9:5906–11.
70. Lussier F, Brulé T, Vishwakarma M, Das T, Spatz JP, Masson J-F. Dynamic SERS optophysiology: A nanosensor for monitoring cell secretion events. *Nano Lett*. 2016;16:3866–71.
71. Cabello G, Nwoko KC, Marco JF, Sánchez-Arenillas M, Méndez-Torres AM, Feldmann J, et al. Cu@Au self-assembled nanoparticles as SERS-active substrates for (bio)molecular sensing. *J Alloy Compd*. 2019;791:184–92.
72. Majumdar D, Singha A, Mondal PK, Kundu S. DNA-mediated wirelike clusters of silver nanoparticles: An ultrasensitive SERS substrate. *ACS Appl Mater Interfaces*. 2013;5:7798–807.
73. Khlebtsov B, Khanadeev V, Khlebtsov N. Surface-enhanced Raman scattering inside Au@Ag core/shell nanorods. *Nano Res*. 2016;9:2303–18.
74. Gao Z, Burrows ND, Valley NA, Schatz GC, Murphy CJ, Haynes CL. In solution SERS sensing using mesoporous silica-coated gold nanorods. *Analyst*. 2016;141:5088–95.
75. Garcia-Leis A, Garcia-Ramos JV, Sanchez-Cortes S. Silver nanostars with high SERS performance. *J Phys Chem C*. 2013;117:7791–5.
76. Niu W, Chua YAA, Zhang W, Huang H, Lu X. Highly symmetric gold nanostars: Crystallographic control and surface-enhanced Raman scattering property. *J Am Chem Soc*. 2015;137:10460–3.
77. Jiang B, Xu L, Chen W, Zou C, Yang Y, Fu Y, et al. Ag<sup>+</sup>-assisted heterogeneous growth of concave Pd@Au nanocubes for surface-enhanced Raman scattering (SERS). *Nano Res*. 2017;10:3509–21.
78. Ben-Jaber S, Peveler WJ, Quesada-Cabrera R, Sol CWO, Papakonstantinou I, Parkin IP. Sensitive and specific detection of explosives in solution and vapour by surface-enhanced Raman spectroscopy on silver nanocubes. *Nanoscale*. 2017;9:16459–66.
79. Wang P, Pang S, Chen J, McLandsborough L, Nugen SR, Fan M, et al. Label-free mapping of single bacterial cells using surface-enhanced Raman spectroscopy. *Analyst*. 2016;141:1356–62.
80. Reyes M, Piotrowski M, Ang SK, Chan J, He S, Chu JJH, et al. Exploiting the anti-aggregation of gold nanostars for rapid detection of hand, foot, and mouth disease causing enterovirus 71 using surface-enhanced Raman spectroscopy. *Anal Chem*. 2017;89:5373–81.
81. Von Maltzahn G, Centrone A, Park JH, Ramanathan R, Sailor MJ, Hatton TA, et al. SERS-coded gold nanorods as a multifunctional platform for densely multiplexed near-infrared imaging and photothermal heating. *Adv Mater*. 2009;21:3175–80.
82. Seo SH, Kim BM, Joe A, Han HW, Chen X, Cheng Z, et al. NIR-light-induced surface-enhanced Raman scattering for detection and photothermal/photodynamic therapy of cancer cells using methylene blue-embedded gold nanorod@SiO<sub>2</sub> nanocomposites. *Biomaterials*. 2014;35:3309–18.
83. Gao Y, Li Y, Wang Y, Chen Y, Gu J, Zhao W, et al. Controlled synthesis of multilayered gold nanoshells for enhanced photothermal therapy and SERS detection. *Small*. 2015;11:77–83.
84. Chen J, Sheng Z, Li P, Wu M, Zhang N, Yu XF, et al. Indocyanine green-loaded gold nanostars for sensitive SERS imaging and subcellular monitoring of photothermal therapy. *Nanoscale*. 2017;9:11888–901.
85. Qi G, Zhang Y, Xu S, Li C, Wang D, Li H, et al. Nucleus and mitochondria targeting theranostic plasmonic surface-enhanced Raman spectroscopy nanoprobes as a means for revealing molecular stress response differences in hyperthermia cell death between cancerous and normal cells. *Anal Chem*. 2018;90:13356–64.
86. Xing Y, Cai Z, Xu M, Ju W, Luo X, Hu Y, et al. Raman observation of a molecular signaling pathway of apoptotic cells induced by photothermal therapy. *Chem Sci*. 2019;10:10900–10.
87. Ali MRK, Wu Y, Han T, Zang X, Xiao H, Tang Y, et al. Simultaneous time-dependent surface-enhanced Raman spectroscopy, metabolomics, and proteomics reveal cancer cell death mechanisms associated with gold nanorod photothermal therapy. *J Am Chem Soc*. 2016;138:15434–42.
88. Gao W, Li B, Yao R, Li Z, Wang X, Dong X, et al. Intuitive label-free SERS detection of bacteria using aptamer-based in situ silver nanoparticles synthesis. *Anal Chem*. 2017;89:9836–42.
89. Wang J, Koo KM, Wee EJH, Wang Y, Trau M. A nanoplasmonic label-free surface-enhanced Raman scattering strategy for non-invasive cancer genetic subtyping in patient samples. *Nanoscale*. 2017;9:3496–503.
90. Alula MT, Krishnan S, Hendricks NR, Karamchand L, Blackburn JM. Identification and quantitation of pathogenic bacteria via in-situ formation of silver nanoparticles on cell walls, and their detection via SERS. *Microchim Acta*. 2017;184:219–27.
91. Koo KM, Wang J, Richards RS, Farrell A, Yaxley JW, Samarasinghe H, et al. Design and clinical verification of surface-enhanced Raman spectroscopy diagnostic technology for individual cancer risk prediction. *ACS Nano*. 2018;12:8362–71.
92. Hong Y, Li Y, Huang L, He W, Wang S, Wang C, et al. Label-free diagnosis for colorectal cancer through coffee ring-assisted surface-enhanced Raman spectroscopy on blood serum. *J Biophotonics*. 2020;13:e201960176.
93. He S, Kyaw YME, Tan EKM, Bekale L, Kang MWC, Kim SSS, et al. Quantitative and label-free detection of protein kinase A activity based on surface-enhanced Raman spectroscopy with gold nanostars. *Anal Chem*. 2018;90:6071–80.
94. Prakash O, Sil S, Verma T, Umapathy S. Direct detection of bacteria using positively charged Ag/Au bimetallic nanoparticles: A label-free surface-enhanced Raman scattering study coupled with multivariate analysis. *J Phys Chem C*. 2020;124:861–9.
95. Wang C, Wang J, Li M, Qu X, Zhang K, Rong Z, et al. A rapid SERS method for label-free bacteria detection using polyethyleneimine-modified Au-coated magnetic microspheres and Au@Ag nanoparticles. *Analyst*. 2016;141:6226–38.
96. Fraire JC, Stremersch S, Bouckaert D, Monteyne T, De Beer T, Wuytens P, et al. Improved label-free identification of individual exosome-like vesicles with Au@Ag nanoparticles as SERS substrate. *ACS Appl Mater Interfaces*. 2019;11:39424–35.
97. Karthick Kannan P, Shankar P, Blackman C, Chung CH. Recent advances in 2D inorganic nanomaterials for SERS sensing. *Adv Mater*. 2019;31:1803432.
98. Kim YK, Kim S, Cho S-P, Jang H, Huh H, Hong BH, et al. Facile one-pot photosynthesis of stable Ag@graphene oxide nanocolloid core@shell nanoparticles with sustainable localized surface plasmon resonance properties. *J Mater Chem C*. 2017;5:10016–22.
99. Zeng F, Xu D, Zhan C, Liang C, Zhao W, Zhang J, et al. Surfactant-free synthesis of graphene oxide coated silver nanoparticles for SERS biosensing and intracellular drug delivery. *ACS Appl Nano Mater*. 2018;1:2748–53.
100. Zhou Y, Huang J, Shi W, Li Y, Wu Y, Liu Q, et al. Ecofriendly and environment-friendly synthesis of size-controlled silver nanoparticles/graphene composites for antimicrobial and SERS actions. *Appl Surf Sci*. 2018;457:1000–8.
101. Meng X, Wang H, Chen N, Ding P, Shi H, Zhai X, et al. A graphene–silver nanoparticle–silicon sandwich SERS chip for quantitative detection of molecules and capture, discrimination, and inactivation of bacteria. *Anal Chem*. 2018;90:5646–53.
102. Huang D, Zhuang Z, Wang Z, Li S, Zhong H, Liu Z, et al. Black phosphorus–Au filter paper-based three-dimensional SERS substrate for rapid detection of foodborne bacteria. *Appl Surf Sci*. 2019;497: 143825.
103. Henan Z, Wen Z, Zhiming L, Deqiu H, Wolun Z, Binggang Y, et al. Insights into the intracellular behaviors of black-phosphorus-based nanocomposites via surface-enhanced Raman spectroscopy. *Nanophotonics*. 2018;7:1651–62.
104. Yang G, Liu Z, Li Y, Hou Y, Fei X, Su C, et al. Facile synthesis of black phosphorus–Au nanocomposites for enhanced photothermal cancer therapy and surface-enhanced Raman scattering analysis. *Biomater Sci*. 2017;5:2048–55.
105. Li D, Yu H, Guo Z, Li S, Li Y, Guo Y, et al. SERS analysis of carcinoma-associated fibroblasts in a tumor microenvironment based on targeted 2D nanosheets. *Nanoscale*. 2020;12:2133–41.
106. Wang J, Liu R, Zhang C, Han G, Zhao J, Liu B, et al. Synthesis of g-C<sub>3</sub>N<sub>4</sub> nanosheet/Au@Ag nanoparticle hybrids as SERS probes for cancer cell diagnostics. *RSC Adv*. 2015;5:86803–10.
107. Wang YN, Zhang Y, Zhang WS, Xu ZR. A SERS substrate of mesoporous g-C<sub>3</sub>N<sub>4</sub> embedded with in situ grown gold



- nanoparticles for sensitive detection of 6-thioguanine. *Sensors Actuat B Chem.* 2018;260:400–7.
108. Zhang H, Zhang W, Gao X, Man P, Sun Y, Liu C, et al. Formation of the AuNPs/GO@MoS<sub>2</sub>/AuNPs nanostructures for the SERS application. *Sensors Actuat B Chem.* 2019;282:809–17.
109. Liu J, Zheng T, Tian Y. Functionalized h-BN nanosheets as a theranostic platform for SERS real-time monitoring of microRNA and photodynamic therapy. *Angew Chem Int Ed.* 2019;58:7757–61.
110. Pramanik A, Davis D, Patibandla S, Begum S, Ray P, Gates K, et al. A WS<sub>2</sub>-gold nanoparticle heterostructure-based novel SERS platform for the rapid identification of antibiotic-resistant pathogens. *Nanoscale Adv.* 2020;2:2025–33.
111. Kavyani S, Dadvar M, Modarress H, Amjad-Iranagh S. Molecular perspective mechanism for drug loading on carbon nanotube-dendrimer: A coarse-grained molecular dynamics study. *J Phys Chem B.* 2018;122:7956–69.
112. Dinda S, Mandal D, Sarkar S, Das PK. Self-assembled vesicle-carbon nanotube conjugate formation through a boronate-diol covalent linkage. *Chem Eur J.* 2017;23:15194–202.
113. Liu H, Li Y, Dykes J, Gilliam T, Burnham K, Chopra N. Manipulating the functionalization surface of graphene-encapsulated gold nanoparticles with single-walled carbon nanotubes for SERS sensing. *Carbon.* 2018;140:306–13.
114. Yang Z, Tian J, Yin Z, Cui C, Qian W, Wei F. Carbon nanotube- and graphene-based nanomaterials and applications in high-voltage supercapacitor: A review. *Carbon.* 2019;141:467–80.
115. Gupta S, Murthy CN, Prabha CR. Recent advances in carbon nanotube-based electrochemical biosensors. *Int J Biol Macromol.* 2018;108:687–703.
116. Rong G, Corrie SR, Clark HA. In vivo biosensing: Progress and perspectives. *ACS Sens.* 2017;2:327–38.
117. Chen Y-C, Young RJ, Macpherson JV, Wilson NR. Silver-decorated carbon nanotube networks as SERS substrates. *J Raman Spectrosc.* 2011;42:1255–62.
118. Qin X, Si Y, Wang D, Wu Z, Li J, Yin Y. Nanoconjugates of Ag/Au/carbon nanotube for alkyne-mediated ratiometric SERS imaging of hypoxia in hepatic ischemia. *Anal Chem.* 2019;91(7):4529–36.
119. Jie Z, Zenghe Y, Xiaolei Z, Yong Z. Quantitative SERS by electromagnetic enhancement normalization with carbon nanotube as an internal standard. *Opt Express.* 2018;26:23534–9.
120. Teresa D, Rajasheshkar K, Zhen F, Anant K-S, Dulal S, Madan D, Eugene Z, Paresh C-R. Highly efficient SERS substrate for direct detection of explosive TNT using popcorn-shaped gold nanoparticle-functionalized SWCNT hybrid. *Analyst.* 2012;137:5041–5.
121. Wei H-N, Peng Z-S, Yang C, Tian Y, Sun L-F, Wang G-T, Liu M. Three-dimensional Au/Ag nanoparticle/crossed carbon nanotube SERS substrate for the detection of mixed toxic molecules. *Nanomaterials.* 2021;11:2026.
122. Cheng H, Zhao Y, Fan Y, Xie X, Qu L, Shi G. Graphene-quantum-dot assembled nanotubes: A new platform for efficient Raman enhancement. *ACS Nano.* 2012;6:2237–44.
123. Liu D, Chen X, Hu Y, Sun T, Song Z, Zheng Y, et al. Raman enhancement on ultra-clean graphene quantum dots produced by quasi-equilibrium plasma-enhanced chemical vapor deposition. *Nat Commun.* 2018;9:193.
124. Bhunia SK, Zeiri L, Manna J, Nandi S, Jelinek R. Carbon-dot/silver-nanoparticle flexible SERS-active films. *ACS Appl Mater Interfaces.* 2016;8:25637–43.
125. Fei X, Liu Z, Hou Y, Li Y, Yang G, Su C, et al. Synthesis of Au NP@MoS<sub>2</sub> quantum dots core@shell nanocomposites for SERS bio-analysis and label-free bio-imaging. *Materials.* 2017;10:650.
126. Pilot R, Signorini R, Durante C, Orian L, Bhamidipati M, Fabris L. A review on surface-enhanced Raman scattering. *Biosens.* 2019;9:57.
127. Zhao X, Li M, Xu Z. Detection of foodborne pathogens by surface-enhanced Raman spectroscopy. *Front Microbiol.* 2018;9:1236.
128. Li J, Dong S, Tong J, Zhu P, Diao G, Yang Z. 3D ordered silver nanoshells silica photonic crystal beads for multiplex encoded SERS bioassay. *Chem Commun.* 2016;52:284–7.
129. Cho WJ, Kim Y, Kim JK. Ultrahigh-density array of silver nanoclusters for SERS substrate with high sensitivity and excellent reproducibility. *ACS Nano.* 2012;6:249–55.
130. Lee SY, Kim SH, Kim MP, Jeon HC, Kang H, Kim HJ, et al. Freestanding and arrayed nanoporous microcylinders for highly active 3D SERS substrate. *Chem Mater.* 2013;25:2421–6.
131. Xie X, Pu H, Sun DW. Recent advances in nanofabrication techniques for SERS substrates and their applications in the food safety analysis. *Crit Rev Food Sci Nutr.* 2018;58:2800–13.
132. Lao Z, Hu Y, Wu D. Fabricating nanogap for SERS by combing laser printing with capillary-force self-assembly on soft base. *OSA Technical Digest (Optica Publishing Group, 2019).* Hawaii United States; 2019. paper NTu4A.8.
133. Fan M, Andrade GFS, Brolo AG. A review on the fabrication of substrates for surface-enhanced Raman spectroscopy and their applications in analytical chemistry. *Anal Chim Acta.* 2011;693:7–25.
134. Jiao T, Yan X, Balan L, Stepanov AL, Chen X, Hu MZ. Chemical functionalization, self-assembly, and applications of nanomaterials and nanocomposites. *J Nanomater.* 2014;2014: 291013.
135. Zhao X, Wen J, Zhang M, Wang D, Wang Y, Chen L, et al. Design of hybrid nanostructural arrays to manipulate SERS-active substrates by nanosphere lithography. *ACS Appl Mater Interfaces.* 2017;9:7710–6.
136. Fang X, Zheng C, Yin Z, Wang Z, Wang J, Liu J, et al. Hierarchically ordered silicon metastructures from improved self-assembly-based nanosphere lithography. *ACS Appl Mater Interfaces.* 2020;12:12345–52.
137. Petti L, Capasso R, Rippl M, Pannico M, La Manna P, Peluso G, et al. A plasmonic nanostructure fabricated by electron beam lithography as a sensitive and highly homogeneous SERS substrate for bio-sensing applications. *Vib Spectrosc.* 2016;82:22–30.
138. Hasna K, Antony A, Puiggollers J, Kumar KR, Jayaraj MK. Fabrication of cost-effective, highly reproducible large area arrays of nanotriangular pillars for surface-enhanced Raman scattering substrates. *Nano Res.* 2016;9:3075–83.
139. Liu TY, Tsai K-T, Wang H-H, Chen Y, Chen Y-H, Chao Y-C, et al. Functionalized arrays of Raman-enhancing nanoparticles for capture and culture-free analysis of bacteria in human blood. *Nat Commun.* 2011;2:538.
140. Im H, Bantz KC, Lee SH, Johnson TW, Haynes CL, Oh S-H. Self-assembled plasmonic nanoring cavity arrays for SERS and LSPR biosensing. *Adv Mater.* 2013;25:2678–85.
141. Rippl M, Castagna R, Pannico M, Musto P, Borriello G, Paradiso R, et al. Octupolar metastructures for a highly sensitive, rapid, and reproducible phage-based detection of bacterial pathogens by surface-enhanced Raman scattering. *ACS Sens.* 2017;2:947–54.
142. Kumar S, Lodhi DK, Goel P, Neeti P, Mishra P, Singh JP. A facile method for fabrication of buckled PDMS silver nanorod arrays as active 3D SERS cages for bacterial sensing. *Chem Commun.* 2015;51:12411–4.
143. Paccotti N, Boschetto F, Horiguchi S, Marin E, Chiadò A, Novara C, et al. Label-free SERS discrimination and in situ analysis of life cycle in *Escherichia coli* and *Staphylococcus epidermidis*. *Biosensors.* 2018;8:131.
144. Zhang Y, Zeng Q, Li L, Qi M, Qi Q, Li S, et al. Characterization and identification of lung cancer cells from blood cells with label-free surface-enhanced Raman scattering. *Laser Phys.* 2019;29: 045602.
145. Shanmukh S, Jones L, Driskell J, Zhao Y, Dluhy R, Tripp RA. Rapid and sensitive detection of respiratory virus molecular signatures using a silver nanorod array SERS substrate. *Nano Lett.* 2006;6:2630–6.
146. Kahraman M, Wachsmann-Hogiu S. Label-free and direct protein detection on 3D plasmonic nanovoid structures using surface-enhanced Raman scattering. *Anal Chim Acta.* 2015;856:74–81.
147. Guselnikova O, Postnikov P, Pershina A, Svorcik V, Lyutakov O. Express and portable label-free DNA detection and recognition with SERS platform based on functional Au grating. *Appl Surf Sci.* 2019;470:219–27.
148. Zhang B, Wang H, Lu L, Ai K, Zhang G, Cheng X. Large-area silver-coated silicon nanowire arrays for molecular sensing using surface-enhanced Raman spectroscopy. *Adv Funct Mater.* 2008;18:2348–55.
149. Nam W, Ren X, Tali SAS, Ghassemi P, Kim I, Agah M, et al. Refractive-index-insensitive nanolaminated SERS substrates for label-free Raman profiling and classification of living cancer cells. *Nano Lett.* 2019;19:7273–81.
150. Plou J, García I, Charconnet M, Astobiza I, García-Astrain C, Matricardi C, et al. Multiplex SERS detection of metabolic alterations in tumor extracellular media. *Adv Funct Mater.* 2020;30:1910335.
151. Ensikat HJ, Ditsche-Kuru P, Neinhuis C, Barthlott W. Superhydrophobicity in perfection: the outstanding properties of the lotus leaf. *Beilstein J Nanotech.* 2011;2:152–61.

152. Feng L, Zhang Y, Li M, Zheng Y, Shen W, Jiang L. The structural color of red rose petals and their duplicates. *Langmuir*. 2010;26:14885–8.
153. Vértesy Z, Bálint Z, Kertész K, Vigneron JP, Lousse V, Biró LP. Wing scale microstructures and nanostructures in butterflies — natural photonic crystals. *J Microsc*. 2006;224:108–10.
154. Autumn K, Sitti M, Liang YA, Peattie AM, Hansen WR, Sponberg S, et al. Evidence for van der Waals adhesion in gecko setae. *Proc Natl Acad Sci*. 2002;99:12252.
155. Huang J-A, Zhang Y-L, Zhao Y, Zhang X-L, Sun M-L, Zhang W. Superhydrophobic SERS chip based on an Ag coated natural taro-leaf. *Nanoscale*. 2016;8:11487–93.
156. Chou S-Y, Yu C-C, Yen Y-T, Lin K-T, Chen H-L, Su W-F. Romantic story or Raman scattering? Rose petals as ecofriendly, low-cost substrates for ultrasensitive surface-enhanced Raman scattering. *Anal Chem*. 2015;87:6017–24.
157. Shao F, Lu Z, Liu C, Han H, Chen K, Li W, et al. Hierarchical nanogaps within bioscaffold arrays as a high-performance SERS substrate for animal virus biosensing. *ACS Appl Mater Interfaces*. 2014;6:6281–9.
158. Tan Y, Gu J, Xu W, Chen Z, Liu D, Liu Q, et al. Reduction of CuO butterfly wing scales generates Cu SERS substrates for DNA base detection. *ACS Appl Mater Interfaces*. 2013;5:9878–82.
159. Du J, Cui J, Jing C. Rapid in situ identification of arsenic species using a portable Fe<sub>3</sub>O<sub>4</sub>@Ag SERS sensor. *Chem Commun*. 2014;50:347–9.
160. Jiang X, Sang Q, Yang M, Du J, Wang W, Wang L, et al. Metal-free SERS substrate based on rGO–TiO<sub>2</sub>–Fe<sub>3</sub>O<sub>4</sub> nanohybrid: contribution from interfacial charge transfer and magnetic controllability. *Phys Chem Chem Phys*. 2019;21:12850–8.
161. Huy LT, Tam LT, Van Son T, Cuong ND, Nam MH, Vinh LK, et al. Photochemical decoration of silver nanocrystals on magnetic MnFe<sub>2</sub>O<sub>4</sub> nanoparticles and their applications in antibacterial agents and SERS-based detection. *J Electron Mater*. 2017;46:3412–21.
162. Yang X, He Y, Wang X, Yuan R. A SERS biosensor with magnetic substrate CoFe<sub>2</sub>O<sub>4</sub>@Ag for sensitive detection of Hg<sup>2+</sup>. *Appl Surf Sci*. 2017;416:581–6.
163. Ding Q, Ma Y, Ye Y, Yang L, Liu J. A simple method to prepare the magnetic Ni@Au core-shell nanostructure for the cycle surface-enhanced Raman scattering substrates. *J Raman Spectrosc*. 2013;44:987–93.
164. Xu X, Li H, Hasan D, Ruoff RS, Wang AX, Fan DL. Near-field enhanced plasmonic-magnetic bifunctional nanotubes for single cell bioanalysis. *Adv Funct Mater*. 2013;23:4332–8.
165. Hardiansyah A, Chen A-Y, Liao H-L, Yang M-C, Liu T-Y, Chan T-Y, et al. Core-shell of FePt@SiO<sub>2</sub>-Au magnetic nanoparticles for rapid SERS detection. *Nanoscale Res Lett*. 2015;10:412.
166. Wang Y, Liu Q, Sun Y, Wang R. Magnetic field modulated SERS enhancement of CoPt hollow nanoparticles with sizes below 10 nm. *Nanoscale*. 2018;10:12650–6.
167. Choi JY, Kim K, Shin KS. Surface-enhanced Raman scattering is inducible by recyclable Ag-coated magnetic particles. *Vib Spectrosc*. 2010;53:117–20.
168. Fan Z, Senapati D, Khan SA, Singh AK, Hamme A, Yust B, et al. Popcorn-shaped magnetic core-plasmonic shell multifunctional nanoparticles for the targeted magnetic separation and enrichment, label-free SERS imaging, and photothermal destruction of multidrug-resistant bacteria. *Chem Eur J*. 2013;19:2839–47.
169. Wang C, Li P, Wang J, Rong Z, Pang Y, Xu J, et al. Polyethylenimine-interlayered core-shell-satellite 3D magnetic microspheres as versatile SERS substrates. *Nanoscale*. 2015;7:18694–707.
170. Han B, Choi N, Kim KH, Lim DW, Choo J. Application of silver-coated magnetic microspheres to a SERS-based optofluidic sensor. *J Phys Chem C*. 2011;115:6290–6.
171. Wang C, Wang J, Li P, Rong Z, Jia X, Ma Q, et al. Sonochemical synthesis of highly branched flower-like Fe<sub>3</sub>O<sub>4</sub>@SiO<sub>2</sub>@Ag microcomposites and their application as versatile SERS substrates. *Nanoscale*. 2016;8:19816–28.
172. Yang T, Guo X, Wu Y, Wang H, Fu S, Wen Y, et al. Facile and label-free detection of lung cancer biomarker in urine by magnetically assisted surface-enhanced Raman scattering. *ACS Appl Mater Interfaces*. 2014;6:20985–93.
173. Zhang J, Gim S, Paris G, Dallabernardina P, Schmitt CNZ, Eickelmann S, et al. Ultrasonic-assisted synthesis of highly defined silver nanodimers by self-assembly for improved surface-enhanced Raman spectroscopy. *Chem Eur J*. 2020;26:1243–8.
174. Purbia R, Nayak PD, Paria S. Visible light-induced Ag nanoparticle deposited urchin-like structures for enhanced SERS application. *Nanoscale*. 2018;10:12970–4.
175. Han XX, Ji W, Zhao B, Ozaki Y. Semiconductor-enhanced Raman scattering: active nanomaterials and applications. *Nanoscale*. 2017;9:4847–61.
176. Keshavarz M, Tan B, Venkatakrishnan K. Label-free SERS quantum semiconductor probe for molecular-level and in vitro cellular detection: A noble-metal-free methodology. *ACS Appl Mater Interface*. 2018;10:34886–904.
177. Kang T, Guan R, Chen X, Song Y, Jiang H, Zhao J. In vitro toxicity of different-sized ZnO nanoparticles in Caco-2 cells. *Nanoscale Res Lett*. 2013;8:496.
178. Han XX, Köhler C, Kozuch J, Kuhlmann U, Paasche L, Sivanesan A, et al. Potential-dependent surface-enhanced resonance Raman spectroscopy at nanostructured TiO<sub>2</sub>: A case study on cytochrome b5. *Small*. 2013;9:4175–81.
179. Lee S, Chon H, Lee J, Ko J, Chung BH, Lim DW, et al. Rapid and sensitive phenotypic marker detection on breast cancer cells using surface-enhanced Raman scattering (SERS) imaging. *Biosens Bioelectron*. 2014;51:238–43.
180. Yang L, Peng Y, Yang Y, Liu J, Li Z, Ma Y, et al. Green and sensitive flexible semiconductor SERS substrates: Hydrogenated black TiO<sub>2</sub> nanowires. *ACS Appl Nano Mater*. 2018;1:4516–27.
181. Wu H, Wang H, Li G. Metal oxide semiconductor SERS-active substrates by defect engineering. *Analyst*. 2017;142:326–35.
182. Chen M, Li K, Luo Y, Shi J, Weng C, Gao L, et al. Improved SERS activity of non-stoichiometric copper sulfide nanostructures related to charge-transfer resonance. *Phys Chem Chem Phys*. 2020;22:5145–53.
183. Zheng Z, Cong S, Gong W, Xuan J, Li G, Lu W, et al. Semiconductor SERS enhancement enabled by oxygen incorporation. *Nat Commun*. 2017;8:1993.
184. Cheng YF, Cao Q, Zhang J, Wu T, Che R. Efficient photodegradation of dye pollutants using a novel plasmonic AgCl microrods array and photo-optimized surface-enhanced Raman scattering. *Appl Catal B: Environ*. 2017;217:37–47.
185. Prasad MD, Krishna MG, Batabyal SK. Facet-engineered surfaces of two-dimensional layered BiOI and Au–BiOI substrates for tuning the surface-enhanced Raman scattering and visible light photodetector response. *ACS Appl Nano Mater*. 2019;2:3906–15.
186. Wang X, Shi W, She G, Mu L. Using Si and Ge nanostructures as substrates for surface-enhanced Raman scattering based on the photoinduced charge transfer mechanism. *J Am Chem Soc*. 2011;133:16518–23.
187. Cui H, Li S, Deng S, Chen H, Wang C. Flexible, transparent, and free-standing silicon nanowire SERS platform for in situ food inspection. *ACS Sens*. 2017;2:386–93.
188. Haldavnekar R, Venkatakrishnan K, Tan B. Non-plasmonic semiconductor quantum SERS probe as a pathway for in vitro cancer detection. *Nat Commun*. 2018;9:3065.
189. Keshavarz M, Kassanos P, Tan B, Venkatakrishnan K. Metal-oxide surface-enhanced Raman biosensor template towards point-of-care EGFR detection and cancer diagnostics. *Nanoscale Horiz*. 2020;5:294–307.
190. Yilmaz M, Babur E, Ozdemir M, Gieseking RL, Dede Y, Tamer U, et al. Nanostructured organic semiconductor films for molecular detection with surface-enhanced Raman spectroscopy. *Nat Mater*. 2017;16:918–24.
191. Demirel G, Gieseking RLM, Ozdemir R, Kahmann S, Loi MA, Schatz GC, et al. Molecular engineering of organic semiconductors enable noble metal-comparable SERS enhancement and sensitivity. *Nat Commun*. 2019;10:5502.
192. Ganesh S, Venkatakrishnan K, Tan B. Quantum scale organic semiconductors for SERS detection of DNA methylation and gene expression. *Nat Commun*. 2020;11:1135.
193. Li Y, Wang Z, Mu X, Ma A, Guo S. Raman tags: Novel optical probes for intracellular sensing and imaging. *Biotechnol Adv*. 2017;35:168–77.
194. Kho KW, Fu CY, Dinis US, Olivo M. Clinical SERS: are we there yet? *J Biophotonics*. 2011;4:667–84.

195. Liu X, Knauer M, Ivleva NP, Niessner R, Haisch C. Synthesis of core-shell surface-enhanced Raman tags for bioimaging. *Anal Chem*. 2010;82:441–6.
196. Yu Q, Wang Y, Mei R, Yin Y, You J, Chen L. Polystyrene encapsulated SERS tags as promising standard tools: Simple and universal in synthesis; highly sensitive and ultrastable for bioimaging. *Anal Chem*. 2019;91:5270–7.
197. Zhang L, Zhang R, Gao M, Zhang X. Facile synthesis of thiol and alkynyl contained SERS reporter molecular and its usage in the assembly of polydopamine protected bioorthogonal SERS tag for live cell imaging. *Talanta*. 2016;158:315–21.
198. Wen S, Miao X, Fan G-C, Xu T, Jiang LP, Wu P, et al. Aptamer-conjugated Au nanocage/SiO<sub>2</sub> core-shell bifunctional nanoprobe with high stability and biocompatibility for cellular SERS imaging and near-infrared photothermal therapy. *ACS Sens*. 2019;4:301–8.
199. Jaworska A, Wojcik T, Malek K, Kwoltek U, Kepczynski M, Ansary AA, et al. Rhodamine 6G conjugated to gold nanoparticles as labels for both SERS and fluorescence studies on live endothelial cells. *Microchim Acta*. 2015;182:119–27.
200. Neng J, Harpster MH, Zhang H, Mechem JO, Wilson WC, Johnson PA. A versatile SERS-based immunoassay for immunoglobulin detection using antigen-coated gold nanoparticles and malachite green-conjugated protein A/G. *Biosens Bioelectron*. 2010;26:1009–15.
201. Song D, Yang R, Fang S, Liu Y, Long F, Zhu A. SERS based aptasensor for ochratoxin A by combining Fe<sub>3</sub>O<sub>4</sub>@Au magnetic nanoparticles and Au-DTNB@Ag nanoprobe with multiple signal enhancement. *Microchim Acta*. 2018;185:491.
202. Simon T, Potara M, Gabudean AM, Licarete E, Banciu M, Astilean S. Designing theranostic agents based on pluronic stabilized gold nanoadgregates loaded with methylene blue for multimodal cell imaging and enhanced photodynamic therapy. *ACS Appl Mater Interfaces*. 2015;7:16191–201.
203. Luo Z, Chen K, Lu D, Han H, Zou M. Synthesis of p-amino thiophenol-embedded gold/silver core-shell nanostructures as novel SERS tags for biosensing applications. *Microchim Acta*. 2011;173:149–56.
204. Shen W, Lin X, Jiang C, Li C, Lin H, Huang J, Wang S, Liu G, Yan X, Zhong Q, Ren B. Reliable quantitative SERS analysis facilitated by core-shell nanoparticles with embedded internal standards. *Angew Chem Int Ed*. 2015;54:7308–12.
205. Loren A, Engelbrektsson J, Eliasson C, Josefson M, Abrahamsson J, Johansson M, Abrahamsson K. Internal standard in surface-enhanced Raman spectroscopy. *Anal Chem*. 2004;76:7391–5.
206. Mei R, Wang Y, Yu Q, Yin Y, Zhao R, Chen L. Gold nanorod array-bridged internal-standard SERS tags: From ultrasensitivity to multifunctionality. *ACS Appl Mater Interfaces*. 2020;12:2059–66.
207. Zou Y, Chen L, Song Z, Ding D, Chen Y, Xu Y, et al. Stable and unique graphitic Raman internal standard nanocapsules for surface-enhanced Raman spectroscopy quantitative analysis. *Nano Res*. 2016;9:1418–25.
208. Zhang J, Zhang X, Chen S, Gong T, Zhu Y. Surface-enhanced Raman scattering properties of multi-walled carbon nanotubes arrays-Ag nanoparticles. *Carbon*. 2016;100:395–407.
209. Justino CIL, Freitas AC, Pereira R, Cuarte AC, Rocha-Santos TAP. Recent developments in recognition elements for chemical sensors and biosensors. *Trends Anal Chem*. 2015;68:2–17.
210. Wang J, Wu X, Wang C, Rong Z, Ding H, Li H, et al. Facile synthesis of Au-coated magnetic nanoparticles and their application in bacteria detection via a SERS method. *ACS Appl Mater Interfaces*. 2016;8:19958–67.
211. Pang Y, Wang C, Xiao R, Sun Z. Dual-selective and dual-enhanced SERS nanoprobe strategy for circulating hepatocellular carcinoma cells detection. *Chem Eur J*. 2018;24:7060–7.
212. Zhang C, Wang C, Xiao R, Tang L, Huang J, Wu D, et al. Sensitive and specific detection of clinical bacteria via vancomycin-modified Fe<sub>3</sub>O<sub>4</sub>@Au nanoparticles and aptamer-functionalized SERS tags. *J Mater Chem B*. 2018;6:3751–61.
213. Zou Y, Huang S, Liao Y, Zhu X, Chen Y, Chen L, et al. Isotopic graphene-isolated-Au-nanocrystals with cellular Raman-silent signals for cancer cell pattern recognition. *Chem Sci*. 2018;9:2842–9.
214. Yin D, Wang S, He Y, Liu J, Zhou M, Ouyang J, et al. Surface-enhanced Raman scattering imaging of cancer cells and tissues via sialic acid-imprinted nanotags. *Chem Commun*. 2015;51:17696–9.
215. Pang Y, Wan N, Shi L, Wang C, Sun Z, Xiao R, et al. Dual-recognition surface-enhanced Raman scattering(SERS) biosensor for pathogenic bacteria detection by using vancomycin-SERS tags and aptamer-Fe<sub>3</sub>O<sub>4</sub>@Au. *Anal Chim Acta*. 2019;1077:288–96.
216. Tang R, Hu R, Jiang X, Lu F. LHRH-targeting surface-enhanced Raman scattering tags for the rapid detection of circulating tumor cells. *Sens Actuat B Chem*. 2019;284:468–74.
217. Zhang Q, Li J, Tang P, Lu X, Tian J, Zhong L. Dynamic imaging of transferrin receptor molecules on single live cell with bridge gaps-enhanced Raman tags. *Nanomaterials*. 2019;9:1373.
218. Wen H, Jiang P, Hu Y, Li G. Synthesis of Au@Ag core-shell nanostructures with a poly(3,4-dihydroxy-L-phenylalanine) interlayer for surface-enhanced Raman scattering imaging of epithelial cells. *Microchim Acta*. 2018;185:353.
219. Beqa L, Fan Z, Singh AK, Senapati D, Ray PC. Gold nano-popcorn attached SWCNT hybrid nanomaterial for targeted diagnosis and photothermal therapy of human breast cancer cells. *ACS Appl Mater Interfaces*. 2011;3:3316–24.
220. Wang X, Wang C, Cheng L, Lee ST, Liu Z. Noble metal coated single-walled carbon nanotubes for applications in surface enhanced Raman scattering imaging and photothermal therapy. *J Am Chem Soc*. 2012;134:7414–22.
221. Kim S, Kim TG, Lee SH, Kim W, Bang A, Moon SW, et al. Label-free surface-enhanced Raman spectroscopy biosensor for on-site breast cancer detection using human tears. *ACS Appl Mater Interfaces*. 2020;12:7897–904.
222. Zhu K, Wang Z, Zong S, Liu Y, Yang K, Li N, et al. Hydrophobic plasmonic nanoacorn array for a label-free and uniform SERS-based biomolecular assay. *ACS Appl Mater Interfaces*. 2020;12:29917–27.
223. Bai XR, Wang LH, Ren JQ, Bai XW, Zeng LW, Shen AG, et al. Accurate clinical diagnosis of liver cancer based on simultaneous detection of ternary specific antigens by magnetic induced mixing surface-enhanced Raman scattering emissions. *Anal Chem*. 2019;91:2955–63.
224. Lin D, Wu Q, Qiu S, Chen G, Feng S, Chen R, et al. Label-free liquid biopsy based on blood circulating DNA detection using SERS-based nanotechnology for nasopharyngeal cancer screening. *Nanomed Nanotechnol*. 2019;22: 102100.
225. Leong SX, Leong YX, Tan EX, Sim HYF, Koh CSL, Lee YH, et al. Non-invasive and point-of-care surface-enhanced Raman scattering (SERS)-based breathalyzer for mass screening of coronavirus disease 2019 (COVID-19) under 5 min. *ACS Nano*. 2022;16:2629–39.
226. Plou J, Valera P-S, Garcia I, Albuquerque CDL, Carracedo A, Marzan LML. Prospects of surface-enhanced Raman spectroscopy for biomarker monitoring toward precision medicine. *ACS Photonics*. 2022;9:333–50.
227. Lussier F, Thibault V, Charron B, Wallace GQ, Masson JF. Deep learning and artificial intelligence methods for Raman and surface-enhanced Raman scattering. *Trend Anal Chem*. 2020;124: 115796.
228. Tang JW, Liu QH, Yin XC, Pan YC, Wen PB, Liu X, et al. Comparative analysis of machine learning algorithms on surface-enhanced Raman spectra of clinical *Staphylococcus* species. *Front Microbiol*. 2021;12: 696921.
229. Huang J, Wen J, Zhou M, Ni S, Le W, Chen G, et al. On-site detection of SARS-CoV-2 antigen by deep learning-based surface-enhanced Raman spectroscopy and its biochemical foundations. *Anal Chem*. 2021;93:9174–82.
230. Shin H, Oh S, Hong S, Kang M, Kang D, Ji Y-G, et al. Early-stage lung cancer diagnosis by deep learning-based spectroscopic analysis of circulating exosomes. *ACS Nano*. 2020;14:5435–44.
231. Lin X, Lin D, Chen Y, Lin J, Weng S, Song J, Feng S. High throughput blood analysis based on deep learning algorithm and self-positioning super-hydrophobic SERS platform for non-invasive multi-disease screening. *Adv Function Mater*. 2021;31:2103382.
232. Uzayisenga V, Lin XD, Li LM, Anema JR, Yang ZL, Huang YF, et al. Synthesis, characterization, and 3D-FDTD simulation of Ag@SiO<sub>2</sub> nanoparticles for shell-isolated nanoparticle-enhanced Raman spectroscopy. *Langmuir*. 2012;28:9140–6.
233. Yang JL, Li RP, Han JH, Huang MJ. FDTD simulation study of size/gap and substrate-dependent SERS activity study of Au@SiO<sub>2</sub> nanoparticles. *Chin Phys B*. 2016;25: 083301.

234. Tira C, Tira D, Simon T, Astilean S. Finite-difference time-domain (FDTD) design of gold nanoparticle chains with specific surface plasmon resonance. *J Mol Struct.* 2014;1072:137–43.
235. Li M, Wang JY, Chen QQ, Lin LH, Radjenovic P, Zhang H, et al. Background-free quantitative surface enhanced Raman spectroscopy analysis using core-shell nanoparticles with an inherent internal standard. *Anal Chem.* 2019;91:15025–31.
236. Shen W, Lin X, Jiang C, Li C, Lin H, Huang J, et al. Reliable quantitative SERS analysis facilitated by core-shell nanoparticles with embedded internal standards. *Angew Chem Int Ed.* 2015;54:7308–12.
237. Rho E, Kim M, Cho SH, Choi B, Park H, Jang H, et al. Separation-free bacterial identification in arbitrary media via deep neural network-based SERS analysis. *Biosens Bioelectron.* 2022;202: 113991.
238. Thrift WJ, Ronaghi S, Samad M, Wei H, Nguyen DG, Cabuslay AS, et al. Deep learning analysis of vibrational spectra of bacterial lysate for rapid antimicrobial susceptibility testing. *ACS Nano.* 2020;14:15336–48.
239. Liu H, Gao X, Xu C, Liu D. SERS tags for biomedical detection and bioimaging. *Theranostics.* 2022;12:1870–903.
240. Qian X, Peng X-H, Ansari DO, Yin-Goen Q, Chen GZ, Shin DM, et al. In vivo tumor targeting and spectroscopic detection with surface-enhanced Raman nanoparticle tags. *Nat Biotechnol.* 2008;26:83–90.
241. Israelsen ND, Hanson C, Vargis E. Nanoparticle properties and synthesis effects on surface-enhanced Raman scattering enhancement factor: An introduction. *Sci World J.* 2015;2015: 124582.
242. Martín C, Kostarelos K, Prato M, Bianco A. Biocompatibility and biodegradability of 2D materials: graphene and beyond. *Chem Commun.* 2019;55:5540–6.
243. Zhang S, Li J, Lykotrafitis G, Bao G, Suresh S. Size-dependent endocytosis of nanoparticles. *Adv Mater.* 2009;21:419–24.
244. Ishigaki M, Maeda Y, Taketani A, Andriana BB, Ishihara R, Wongravee K, et al. Diagnosis of early-stage esophageal cancer by Raman spectroscopy and chemometric techniques. *Analyst.* 2016;141:1027–33.
245. Yeh Y-T, Gulino K, Zhang Y, Sabestien A, Chou T-W, Zhou B, et al. A rapid and label-free platform for virus capture and identification from clinical samples. *P Natl Acad Sci.* 2020;117:895.
246. Moldovan R, Vereshchagina E, Milenko K, Iacob BC, Bodoki AE, Falamas A, et al. Review on combining surface-enhanced Raman spectroscopy and electrochemistry for analytical applications. *Anal Chim Acta.* 2022;1209: 339250.
247. Wang Y, Zhao C, Wang J, Luo X, Xie L, Zhan S, et al. Wearable plasmonic-metasurface sensor for noninvasive and universal molecular fingerprint detection on biointerfaces. *Sci Adv.* 2021;7:eabe4553.
248. Koh EH, Lee WC, Choi YJ, Moon JI, Jang J, Park SG, et al. A Wearable surface-enhanced Raman scattering sensor for label-free molecular detection. *ACS Appl Mater Interfaces.* 2021;13:3024–32.
249. Wang Y, Zhou C, Wang W, Xu D, Zeng F, Zhan C, et al. Photocatalytically powered matchlike nanomotor for light-guided active SERS sensing. *Angew Chem Int Ed.* 2018;57:13110–3.
250. Fan X, Hao Q, Li M, Zhang X, Yang X, Mei Y, et al. Hotspots on the move: Active molecular enrichment by hierarchically structured micro-motors for ultrasensitive SERS sensing. *ACS Appl Mater Interfaces.* 2020;12:28783–91.

## Publisher's Note

Springer Nature remains neutral with regard to jurisdictional claims in published maps and institutional affiliations.

Ready to submit your research? Choose BMC and benefit from:

- fast, convenient online submission
- thorough peer review by experienced researchers in your field
- rapid publication on acceptance
- support for research data, including large and complex data types
- gold Open Access which fosters wider collaboration and increased citations
- maximum visibility for your research: over 100M website views per year

At BMC, research is always in progress.

Learn more [biomedcentral.com/submissions](https://biomedcentral.com/submissions)

